scientific reports

Check for updates

OPEN

Enhancing cardiac disease detection via a fusion of machine learning and medical imaging

Tao Yu[1] & KeYue Chen[2]✉

Cardiovascular illnesses continue to be a predominant cause of mortality globally, underscoring the necessity for prompt and precise diagnosis to mitigate consequences and healthcare expenditures. This work presents a complete hybrid methodology that integrates machine learning techniques with medical image analysis to improve the identification of cardiovascular diseases. This research integrates many imaging modalities such as echocardiography, cardiac MRI, and chest radiographs with patient health records, enhancing diagnosis accuracy beyond standard techniques that depend exclusively on numerical clinical data. During the preprocessing phase, essential visual elements are collected from medical pictures utilizing image processing methods and convolutional neural networks (CNNs). These are subsequently integrated with clinical characteristics and input into various machine learning classifiers, including Support Vector Machines (SVM), Random Forest (RF), XGBoost, and Deep Neural Networks (DNNs), to differentiate between healthy persons and patients with cardiovascular illnesses. The proposed method attained a remarkable diagnostic accuracy of up to 96%, exceeding models reliant exclusively on clinical data. This study highlights the capability of integrating artificial intelligence with medical imaging to create a highly accurate and non-invasive diagnostic instrument for cardiovascular disease.

Keywords AI in medicine, Machine learning, Medical imaging, Cardiovascular disease, Deep learning, Hybrid diagnosis, Echocardiography, Cardiac MRI, Chest radiography

Throughout history, Cardiovascular diseases (CVDs) are among the most significant causes of morbidity and mortality worldwide[1]. Medical research has devoted significant attention to cardiovascular illnesses among these ailments[2,3]. Statistics from the World Health Organization indicate that cardiovascular illnesses are the leading cause of mortality globally and in numerous developed nations, responsible for nearly 47% of deaths, with an individual succumbing to this ailment approximately every 34 s[4–6]. Conversely, in developing nations, a report by the World Health Organization indicates that 11 to 15% of fatalities are attributable to cardiovascular disorders. Based on data from epidemiological research undertaken in these countries in 2023 revealed that of 321,570 deaths, 82,307 were attributable to coronary heart disease, representing 25.6% of total fatalities[7,8]. Cardiologists have recognized numerous physical factors, such as hypertension[9], elevated levels of detrimental cholesterol, diabetes[10], insufficient physical activity, obesity, and genetic predisposition, as contributors to coronary heart disease; however, these factors account for only up to 50% of the disease's incidence, and individually[11], they do not suffice to predict or cause coronary heart disease. Cardiovascular disorders are prevalent conditions that anyone may experience; yet, insufficient understanding of these ailments can lead to their exacerbation, thereby complicating or rendering the treatment procedure unmanageable[12].

Cardiovascular diseases are influenced by various pathological mechanisms, including cancer-induced complications, as demonstrated in a mouse model of lung cancer-induced heart failure[13]. The diagnostic potential of ultrasound imaging is highlighted by its critical role in the treatment of cardiovascular illnesses, especially the stabilization of atherosclerotic plaques[14]; however, because to its high cost, researchers have consistently sought alternate approaches to enhance public awareness and facilitate the timely diagnosis of cardiac conditions[15]. Studies on xanthohumol have demonstrated that pathways including PTEN/Akt/mTOR can affect cardiac fibroblast activation, a critical determinant in cardiovascular disorders[16]. To date, angiography has been the predominant technique for assessing coronary artery disease and diagnosing this condition[17]. Heart diseases such left ventricular hypertrophy are caused by risk factors like weight fluctuations, which highlights the importance of early identification[18]. This intrusive approach entails significant costs

[1]School of Basic Medical Sciences, Zhejiang Chinese Medical University, Hangzhou, ZheJiang, China. [2]Fifth School of Clinical Medicine of Zhejiang Chinese Medical University , Huzhou Cental Hospital, Huzhou, ZheJiang, China. ✉email: keyuechen123@zcmu.edu.cn

for both the patient and medical personnel, and it poses numerous hazards, including mortality, myocardial infarction, and cerebrovascular accident[19]. Currently, machine learning algorithms and neural networks are employed to develop medical models for many applications. The requirement for precise diagnostic instruments is highlighted by advanced interventions, such as subcutaneous cardioverter defibrillators for uncommon heart diseases[20]. Across all sectors, particularly in healthcare, these technologies facilitate the collection, storage, and analysis of data, hence enabling the modeling of diseases, which can significantly assist patients and physicians in the medical field[8,21]. Coronary artery disease is a prevalent cardiac disorder characterized by the accumulation of cholesterol, calcium, and other lipids in the arteries supplying blood to the heart, resulting in arterial obstruction and inadequate blood flow to the heart[22]. The heart is starved of oxygen, resulting in chest pain. Timely detection of this condition is crucial for prevention and management; hence, computer science and artificial intelligence techniques have been extensively employed to assist patients and inform medical decisions.

Examples of machine learning applications in cardiac imaging are depicted in Fig. 1, covering tasks like automatic report generation in cardiac ultrasonography, calcium deposit detection in CT, and left ventricular segmentation in MRI. In keeping with the current study's objective of using a mix of image and clinical data to more reliably detect cardiac illnesses, this picture depicts the extensive application of convolutional neural networks (CNNs) in medical imaging. In the current study, image data from cardiac MRI and echocardiography is combined with clinical information and analyzed in a multi-model machine learning architecture using similar image processing and feature extraction techniques to develop a non-invasive and precise system for diagnosing cardiac diseases.

Cardiovascular disorders, the largest cause of death worldwide, must be diagnosed early. In wealthy countries, these diseases kill one person every 34 s, highlighting the necessity for precise, fast, and non-invasive diagnostic procedures. Angiography is effective, but its high costs, hazards, and limited accessibility make it unsuitable for universal screening and early detection. This research aims to build a cost-effective and precise hybrid approach using artificial intelligence and medical image analysis to improve heart disease diagnosis and public health management.

This research is unique in its seamless integration of medical imaging data (echocardiography, cardiac MRI, and chest X-rays) with clinical data in a hybrid architecture powered by machine learning and deep neural networks. This study uses advanced image processing techniques, including convolutional neural networks

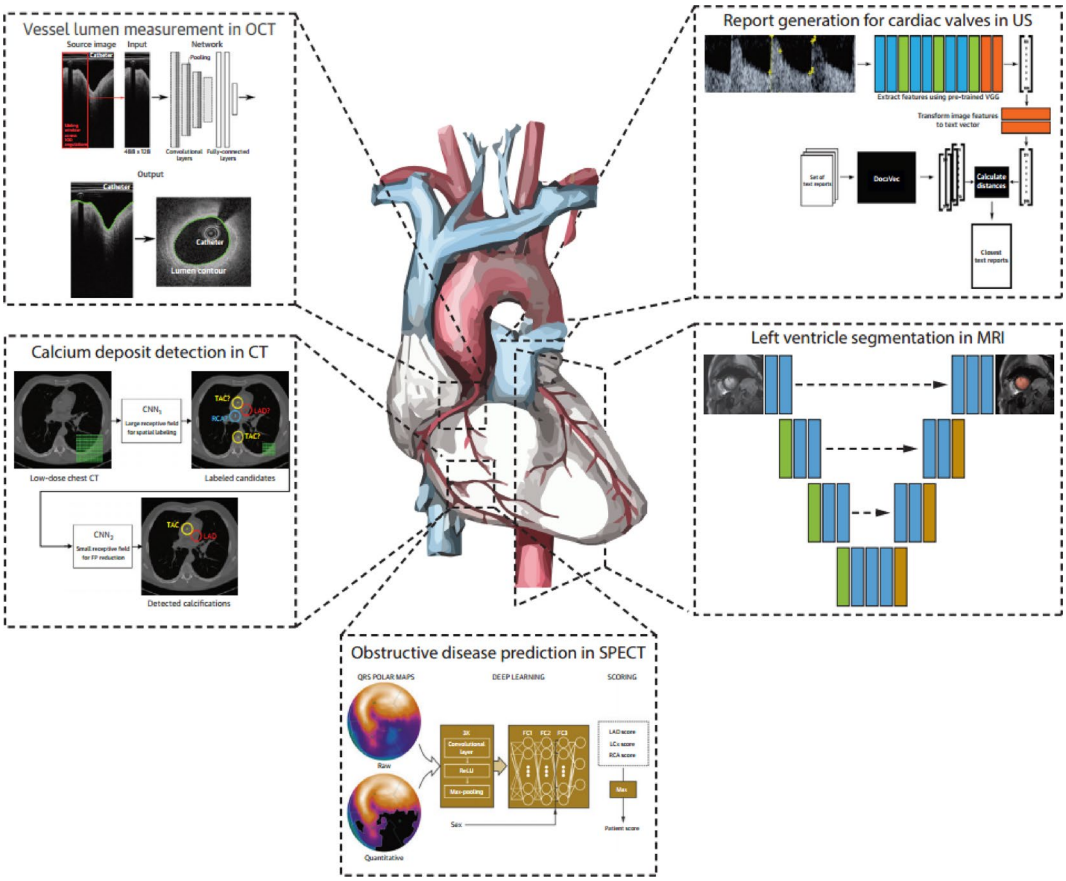

Fig. 1. Applications of cardiac imaging using machine learning. This figure shows examples of applications of machine learning in cardiac imaging, including automated report generation in cardiac ultrasound, identification of calcium deposits in CT scans, and left ventricular segmentation in MRI.

(CNNs), to extract relevant characteristics from medical images and merge them with clinical variables, unlike prior studies that used numerical patient data.

The use of deep learning-based data discretization algorithms and entropy-driven criteria in data optimization improves predicted accuracy and sets this work apart. This research's main contributions:

- Integrating imaging and clinical data with diverse machine learning models (e.g., SVM, Random Forest, XGBoost, and DNNs) yields diagnostic accuracy of up to 96%, outperforming clinical-only models.
- Multi-source data and advanced processing are used to create a non-invasive diagnosis system that can replace costly and risky procedures like angiography.
- This research improves model performance and clinical decision-making by systematically preparing data using deep learning-based discretization and feature selection criteria like Information Gain.

The rest of the paper is organized as follows. A review of previous work is reported in Sect. 2. Materials and Methods are discussed in Sect. 3. The proposed method is discussed in detail in Sect. 4. Experimental evaluation and results are presented in Sect. 5, and finally, conclusions and future work are reported in Sect. 6.

Related works

AI is becoming critical in medicine, resulting in the rapid development of important diagnostic tools. Deep learning (DL) is heavily employed in medical imaging as a computer vision technology[23]. According to medical literature, DL is commonly employed in medical research. DL is a new topic with potential obstacles, and its use in clinical diagnosis is modest. More diagnostic methods are needed to improve medical image analysis for disease diagnosis. At this point, DL is a black box that demands understanding of its internal workings, presenting technical hurdles that require methodological improvement[24]. A proper diagnosis allows preoperative computer simulation planning to deploy the right surgical intervention technology. Deep learning's use in echocardiography for the diagnosis of cardiac problems has been validated by its successful application to enhance ultrasound imaging, including high-resolution microvascular imaging[25]. It addresses challenges raised by the paradigm shift of AI versus DL in CVD diagnosis, proposes remedies, and predicts the future of associated machine intelligence applications. Modular characteristics of DL are used to illustrate CVD picture classification, segmentation, and detection difficulties.

In line with our hybrid approach, interpretable machine learning models like those utilized for neurocognitive disorders showcase the value of interpretability in medical diagnosis[26]. The study uses 14 primary features from the dataset. With accuracy and confusion matrices, promising results are verified. Separation forest manages irrelevant features and normalizes the data for improved outcomes.

The diagnosis of disease is the paramount function of healthcare. Early detection of an illness, prior to its natural or anticipated progression, can preserve lives. The use of deep learning models in image-based diagnosis has been confirmed by their superior performance in evaluating cardiac sounds for the identification of heart disorders[27]. Consequently, it is an opportune moment for both physicians and patients, as heart disease now ranks among the most perilous and life-threatening conditions globally, mostly due to the challenges associated with its diagnosis. In[28], we present a comprehensive overview of categorization techniques for machine learning and image fusion that have demonstrated efficacy in assisting healthcare practitioners with the identification of heart disorders. Human heart fibroblasts (HCFs) were transformed into CPP-like cells (also known as induced CPPs, or iCPPs) in the study[29], and the therapeutic potential of exosomes produced from iCPP for acute lung injury (ALI) was assessed. Primary passage 3 HCFs overexpressing GLI1, WNT2, ISL1, and TBX5 (GWIT) produced iCPPs. The culture media of passages 6–8 of GWIT-iCPPs was used to isolate exosomes. LPS was injected intratracheally to create a model of ALI in mice. GWIT-iCPP-derived exosomes (5×109, 5×1010 particles/ml) were administered to ALI mice via intratracheal induction four hours after LPS induction.

Cardiovascular disease constitutes a significant challenge in contemporary society and is a primary contributor to global mortality rates. Recent breakthroughs in machine learning (ML) applications have demonstrated the feasibility of early heart disease diagnosis utilizing electrocardiogram (ECG) and patient data. Nonetheless, ECG and patient data frequently exhibit imbalance, which eventually presents a problem for conventional machine learning to operate impartially[30]. Numerous data-level and algorithm-level solutions have been presented by various scholars and experts throughout the years. Our researchers found that Gli1 facilitates the spread of NSCLC in[31]. Gli1 expression was linked to a lower chance of survival for patients with non-small cell lung cancer. While downregulating Gli1 in high-metastatic NCI-H1299 and NCI-H1703 cells had the opposite effect, aberrant expression of Gli1 in low-metastatic A549 and NCI-H460 cells enhanced their capacity for migration and invasion and aided the EMT process. Researchers in[32] came up with a machine learning (ML) model that can accurately and realistically predict the passive properties of the heart muscle based on a few geometric, architectural, and hemodynamic criteria. This avoids the long steps that are usually needed in inverse cardiac finite element problems. We designed the geometric features and fiber orientations such that they could be easily seen in normal cardiac imaging methods. Historically, these data were utilized in isolation; however, contemporary machine learning (ML) and deep learning (DL) technologies facilitate the integration of these data sources to produce multimodal insights. Data fusion, which amalgamates information from several modalities through machine learning and deep learning methodologies, has garnered heightened interest in its medical applications. Researchers used a multilayer perceptron artificial neural network, which incorporates a genetic algorithm and an error propagation mechanism, to assess two cardiac disorders in[33]. Given the growing amount of patient data and the pervasive usage of electronic clinical records, artificial neural networks' capacity to process sequential time series data is essential for resource efficiency in intelligent e-health systems. To do this, more precise prediction models must be created. The suggested system uses Internet of Things (IoT) sensors to

gather data, which is then used to do predictive analysis on cloud-stored electronic healthcare data related to patient records.

Researchers in[34] looked studied how accurate and useful three machine learning (ML) models were for predicting the properties of myocardial material using anatomical and hemodynamic parameters directly, without having to solve a complicated FE problem. We generated a fake dataset of 2000 heart samples for training. It used MRI data from 25 mouse hearts, including healthy mice and mice with heart attacks and high blood pressure in the lungs.

A machine learning (ML) model that only uses cardiac stresses as input has led to the development of a completely non-invasive way to find the location and amount of infarcted areas in the left ventricle in[35]. In this groundbreaking study, a multi-fidelity machine learning model that combines training data from rodent-based computer software (which has low accuracy) with very limited patient-specific human data (which has high accuracy) has been shown to be very good at predicting the ground truth of LGE.

Materials and methods

In this section, the methods and algorithms used in this research are introduced. Algorithms in this field are classified into two distinct categories: algorithms used in modeling and algorithms used in data processing.

The raw image of the original cardiac ultrasound data, which displays the ventricles and atria together with the noise and unprocessed features captured by the imaging device, is displayed on the left side of Fig. 2. This picture serves as the first input for the suggested method of diagnosing heart disease. The segmented image on the right illustrates the outcome of using preprocessing and segmentation techniques like the U-Net model and full convolutional networks (FCN), which separate and highlight important heart areas like the left ventricle from the background. This shape serves as input and output data for the image enhancement and segmentation process, as per the method suggested in the paper. The raw image is first processed using a Gaussian filter to eliminate noise and normalize pixel intensity to the interval [0,1], and then it is segmented using deep learning models to extract more precise features and increase the diagnosis accuracy of heart disease.

Data processing

In this study, with the aim of improving the accuracy of heart disease diagnosis, the data used consists of two main categories: clinical data (counts) and medical images (such as echocardiography, cardiac MRI, and chest X-ray). First, the medical images are enhanced through a series of preprocessing steps[35]; these images are optimized in terms of exposure, contrast, and noise removal, and then the diversity and size of the training samples are increased using data augmentation techniques such as rotation, scaling, and random cropping. In the next step, using convolutional neural networks (CNNs) and pre-trained models such as Res Net, Dense Net, and Efficient Net, meaningful features are extracted from the images and converted into feature vectors, which are used as input to classification models in subsequent analyses. To improve the quality of medical images, techniques such as low-light image enhancement based on virtual exposure were used to enhance clarity and extract features[36]. At the same time, clinical data including indicators such as blood pressure, cholesterol levels, and other clinical features are processed after removing outliers and normalizing (using methods such as Min-

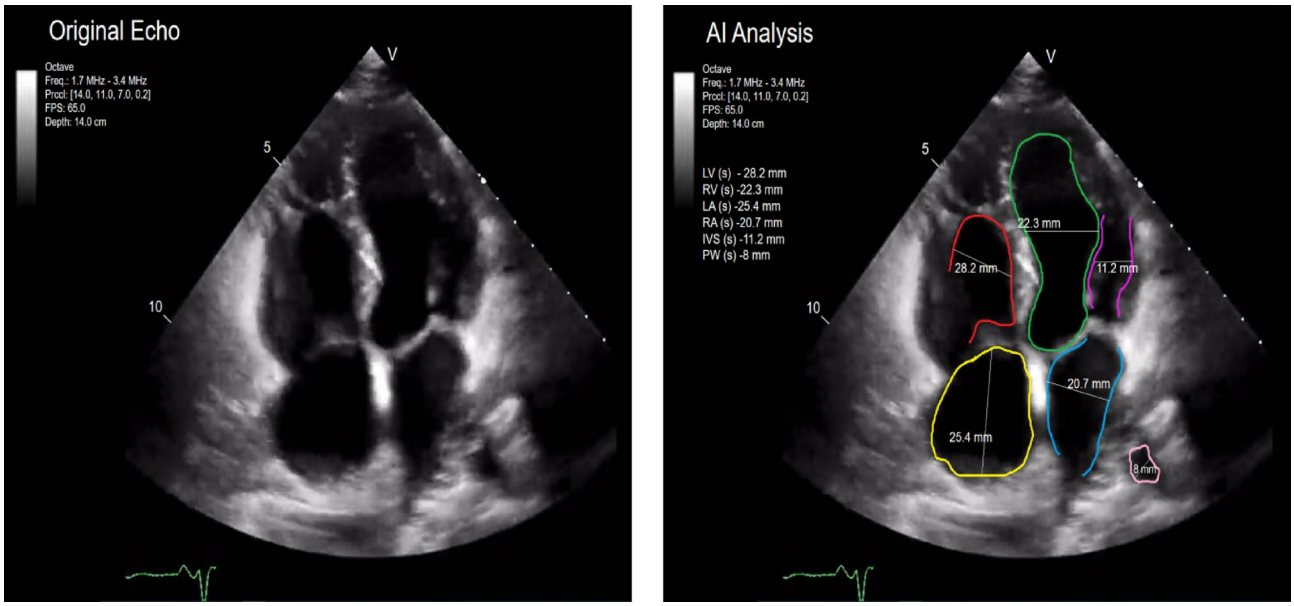

Fig. 2. Cardiac ultrasound image and preprocessing steps. The raw cardiac ultrasound image on the left, which includes the ventricles, atria, and imaging device noise, and the segmented image on the right, which is the result of using preprocessing and segmentation techniques (such as the U-Net model and full convolutional networks FCN).

Max Scaling or Z-score)[37]. The following procedures were used to process the image data from the EchoNet-Dynamic dataset: In order to enhance the visual quality and precision of feature extraction, the images were first denoised using a Gaussian filter. In order to preserve data homogeneity, the images were then scaled to the interval [0,1] via pixel intensity normalization. Lastly, to concentrate feature extraction on structures pertinent to heart illness, important cardiac regions (such the left ventricle) were segmented using a fully convolutional neural network (FCN) and the U-Net model. To improve the discretization process of this numerical data, instead of using traditional methods such as MDLP, a deep learning-based approach is used. In order to extract important features, the data is first compressed using autoencoders. The compressed data is then split into distinct intervals using clustering methods like K-means, whose parameters are tailored for the dataset. Feature extraction from medical images has been improved using advanced models such as Convolution-Transformer, which combines convolutional and transformer architectures[37]. A multimodal feature extraction framework was used to merge the UCI Cleveland and EchoNet-Dynamic data, which lack common patient identifiers. Clinical features were extracted from the UCI Cleveland data using normalization and discretization techniques such as Min-Max Scaling and deep learning-based methods such as autoencoder and K-means, as described in Eqs. 1–3. Similarly, and based on Table 3, image features were extracted from the EchoNet-Dynamic data using deep learning models such as ResNet-50 and U-Net, which produced features such as left ventricular area and mean pixel intensity. Figure 3 illustrates the step-by-step procedure for combining clinical data (UCI Cleveland) and imaging data (EchoNet-Dynamic) in the suggested multimodal architecture. The picture data was processed by performing noise reduction and segmentation, while the clinical data was first prepared using preprocessing techniques like normalization and discretization based on Eq. 1 to 3 and deep learning-based approaches like autoencoder and K-means. In order to generate feature vectors with specific dimensions, features were extracted using multilayer neural networks for clinical data and ResNet-50 and U-Net models for image data, respectively. Statistical alignment and dimensionality reduction were used to ensure consistency while these vectors were concatenated in a common feature space during the feature fusion step. In order to give metrics for evaluating and predicting heart disease, such as accuracy and AUC, the collected data was then fed into classification models, which in the studies produced the highest accuracy.

To evaluate the quality of discretization, entropy measures are used. The entropy of the data set S is calculated as follows:

$$H(S) = -\sum_{i=1}^{n} P(x_i) \log P(x_i) \tag{1}$$

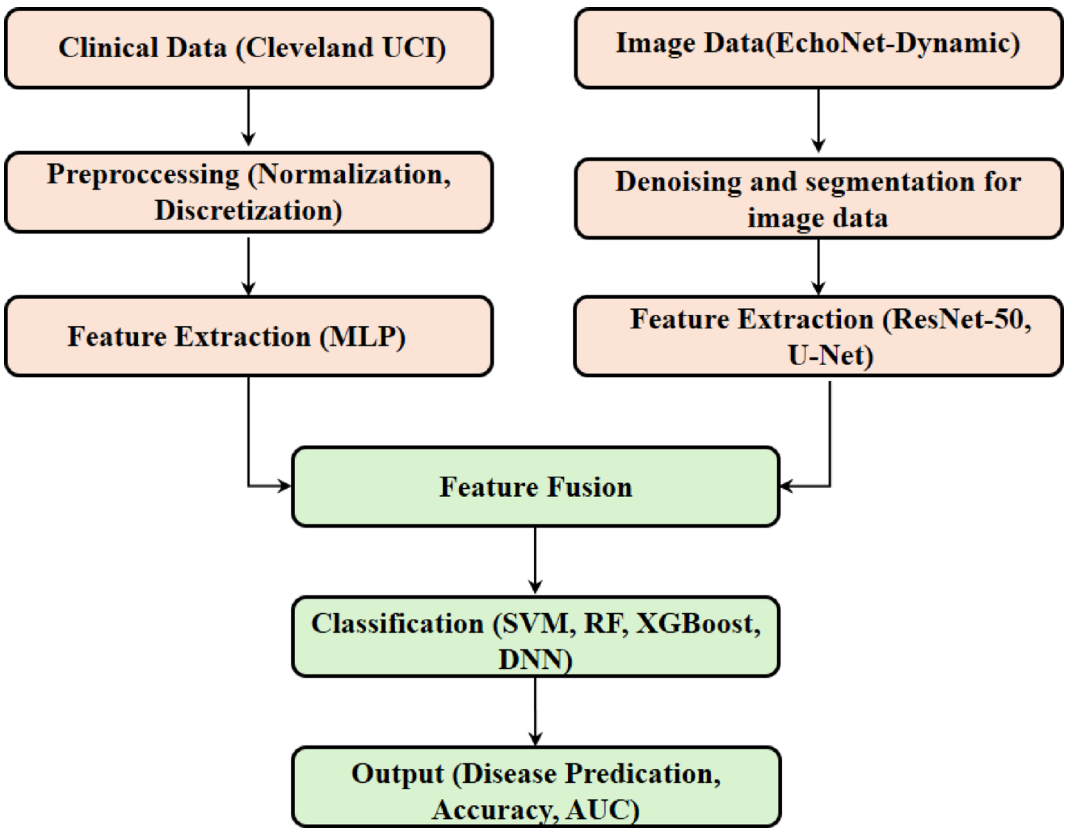

Fig. 3. The process of merging clinical data and image data in the proposed multimodal framework.

where $P(x_i)$ is the probability of occurrence of the value x_i and n is the number of different categories in the set[38]. Also, after discretization, the entropy of the feature A is calculated as follows:

$$H(S,\ A)\ =\ \sum_{v\in\ Values(A)} \frac{|S_v|}{|S|}\ H\ (S_v) \tag{2}$$

In Eq. (2), $|S_v|$ is the number of samples that have the feature A value v and $|S|$ is the total number of samples. In order to select the optimal discretization points, the information Gain criterion is used as the Eq. (3)[39]. The higher the value of $Gain(S,\ A)$, the more important feature A is in reducing uncertainty and should be used in discretizing the data.

$$Gain(S,\ A)\ =\ H\ (S)\ -\ H(S,\ A) \tag{3}$$

The cut point that creates the highest Gain value is selected as the optimal discretization point. In the final stage, the features extracted from medical images and clinical data after deep learning-based discretization are integrated into a multimodal analysis framework. In this framework, advanced models based on Transformer or other multimodal architectures simultaneously process and interpret image and numerical data. Deep learning-based filtering methods were used to denoize echocardiograms in order to enhance picture quality and detection precision[40]. This method involves initially compressing the data with autoencoders to extract significant features, followed by segmenting the compressed data into discrete intervals with clustering methods like K-means, with settings tailored to the dataset. This method, akin to others documented in recent research, can enhance detection accuracy by approximately 96%[41]. The use of entropy and Gain criteria in automatically determining the optimal discretization points reduces errors and accelerates the clinical decision-making process.

Figure 4 shows the proposed architecture of the cardiac disease detection system that combines clinical data from the Cleveland UCI dataset with echocardiogram images from the EchoNet-Dynamic dataset. The preprocessing step of the scheme involves data segmentation using the FCN/U-Net approach to identify heart regions, normalization to the interval [0,1], and noise reduction (using a Gaussian filter). After that, features are extracted from the clinical data using MLP and the EchoNet images using ResNet-50 CNN. These features are then combined using feature fusion, which combines CNN and MLP. ADA Boost/SVM is used for the final classification, and the results are displayed as a diagnosis of the presence or absence of cardiac disease. Figure 4 in the article depicts the architecture of the proposed multi-modal data fusion framework for heart disease detection, visually demonstrating the amalgamation of imaging and clinical data. The diagram is organized in a layered fashion, commencing with the input layer that aggregates several data sources, including medical pictures (echocardiography, cardiac MRI, and chest X-rays) and clinical data (e.g., blood pressure, cholesterol levels, and demographic information). The inputs are subjected to preprocessing in the following layer, where images are refined by techniques such as noise elimination and data augmentation, while clinical data is normalized and

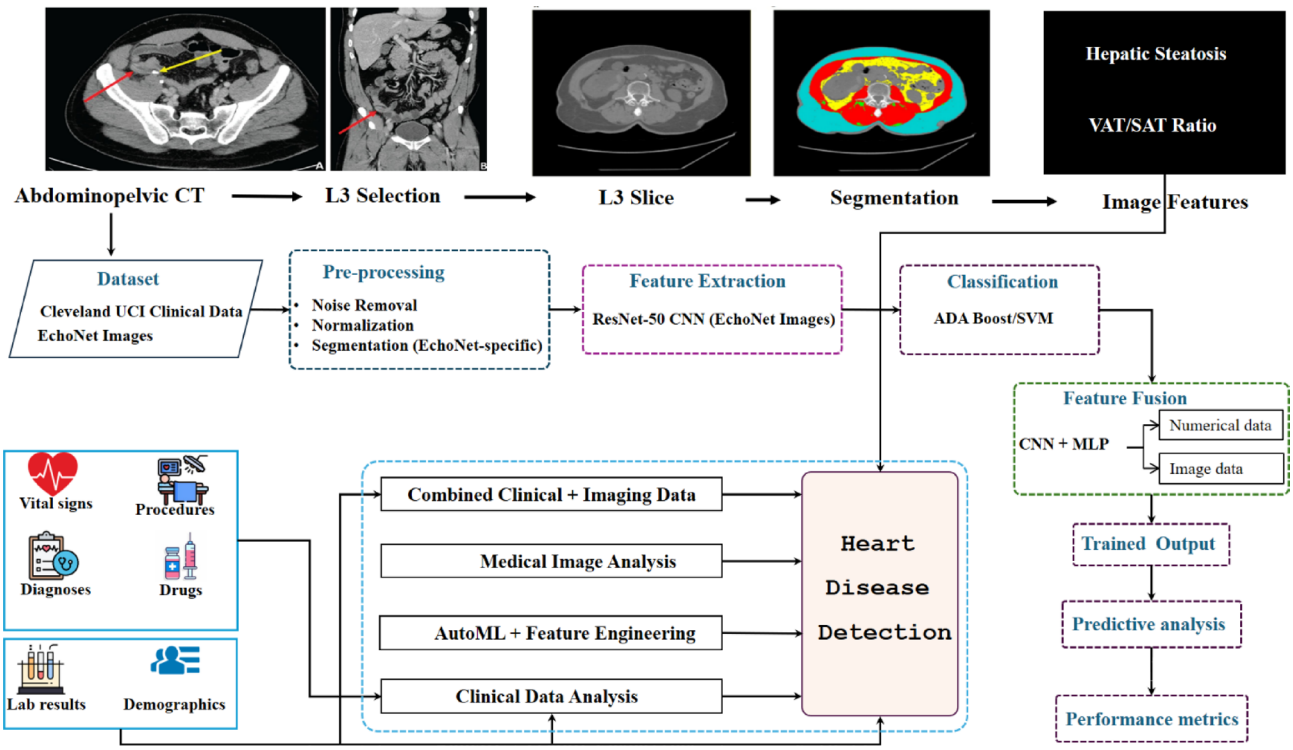

Fig. 4. Architecture of multi-modal data fusion combining Imaging and clinical data.

discretized. The processed data is subsequently input into a feature extraction module, utilizing convolutional neural networks (CNNs) for imaging data and quantitative analysis for clinical data to extract significant features. The features are integrated into a cohesive dataset, which is analyzed by sophisticated machine learning models (e.g., SVM, Random Forest, XGBoost, and DNNs) in the last layer to generate diagnostic outputs, including disease predictions and risk evaluations.

Modeling algorithms

- Decision Tree Algorithm: A decision tree is a prevalent and widely utilized technique in categorization. This algorithm is currently prevalent throughout multiple domains, particularly in medicine[41]. The decision tree framework in machine learning serves as a predictive model and is regarded as one of the most used machine learning techniques. In a decision tree, the leaves signify the classifications, while the branches and intermediary nodes denote the many features that lead to a classification. A decision tree can be depicted using a collection of criteria or rules.
- Random Forest Algorithm: The Random Forest Algorithm is a classification technique regarded as one of the most prevalent and robust ways for addressing huge and intricate issues[42]. This algorithm comprises a collection of decision trees, each casting a vote for each sample, and a subset of trees determines the data class by selecting the category with the highest number of votes.
- XGBoost Algorithm: This algorithm is an enhanced gradient method that excels in classification, regression, and ranking tasks. It is highly regarded in classification tasks for its precise predictions[43], rapid performance, and capability for multi-objective and distributed execution.
- Support Vector Machine Algorithms: A category of supervised machine learning algorithms employed for classification and regression, grounded in statistical learning theory. A support vector machine transforms each data point into a new space based on its class, facilitating linear (hyperplane) categorization[44]. Subsequently, by identifying the support lines of the support planes in multidimensional space, it determines the linear equation that maximizes the distance between the clusters.
- Multilayer Perceptron Neural Network: The Multilayer Perceptron Neural Network is among the most prevalent neural networks available. These networks consist of three layers: input, hidden, and output. In multilayer perceptron networks, input data is transmitted to the input layer to compute the input values for the input neurons[45]. Subsequently, they are transmitted to the concealed layers for processing and ultimately to the neurons of the output layer to compute the network's output value. This network is trained using the error backpropagation algorithm, whereby the computed outputs are compared to the real outputs, allowing for the calculation of the error, which is then utilized to adjust the errors in the intermediate layers. Ultimately, the network weights are adjusted in an effort to minimize the error cost function across various time intervals.

Research data

This work made use of a hybrid dataset that combines image data from the EchoNet-Dynamic dataset with clinical data from the Cleveland Clinic Heart Dataset from the UCI repository (282 samples with 30 clinical variables). More than 10,000 echocardiography videos with heart disease labels make up the EchoNet-Dynamic dataset, which may be downloaded from the company's official website https://echonet.github.io/dynamic[46]. Five hundred image frames from these recordings were chosen and used for this investigation. Table 1 delineates the applicable feature set. It is important to highlight that if the feature requires discretization, following the discretization procedures outlined in Fig. 8 and establishing the suitable interval, the boundaries of each feature are specified in Table 1. The medical limit of the Chol feature was established in, while the T rest BPs and T rest bpd characteristics were determined in[47], and the Thala rest feature in[48].

Proposed research method

This section encompasses the procedures for feature selection, management of missing data, identification and management of outliers, data normalization and discretization, and data visualization to enhance feature recognition. Section 3.3 delineates the modeling procedures, interpretation, and assessment of outcomes.

Data identification phase

This segment of the research requires not only acquiring essential facts regarding the heart and cardiovascular disorders but also evaluating the dataset from both medical and technological viewpoints to ensure its appropriateness for developing a predictive model for heart diseases.

Based on the extensive investigations and research completed on the Cleveland Clinic heart patients data set, it can be determined that this data set is an appropriate selection for developing a model to predict heart disorders.

Furthermore, given that the data utilized in the research comprises authentic information categorized as either sick or healthy by medical professionals and diagnostic tests, it can be inferred that, after developing predictive models and attaining satisfactory accuracy, the results are deemed acceptable from both a medical and technical standpoint, and can be employed to forecast heart diseases.

Data Preparation phase

The features taken from clinical data (Cleveland UCI) and cardiac ultrasound pictures (EchoNet-Dynamic) are contrasted in Table 2. Clinical characteristics like blood pressure and cholesterol are integrated with image features like cardiac region area and mean pixel intensity, which are recovered using FCN and U-Net models and displayed in Figs. 2 and 6.

Name and description of the feature	Type of discrete feature and limit
Age	Less than 51 years, 51 to 59 years, 59 years and above
Sex	Woman: 0, Man: 1
Foamiest (Family background)	Yes: 1, No: 0
Smoking	Yes: 1, No: 0
CP (The kind of chest pain)	- typical angina - atypical angina - non-anginal pain - asymptomatic
Chol (Serum cholesterol) (mg/dl)	Less than 200 mg/dL, 200 to 239 mg/dL, 239 mg/dL and above
FBC (Blood sugar levels) (mg/dl)	0: 120 mg/dL and higher, 1: Under 120 mg/dL
T rest BPs (Blood pressure systolic)	Less than 90 mmHg, 90 to 120 mmHg, 120 to 140 mmHg, 140 mmHg and above
T rest bpd (Blood pressure diastolic)	Less than 60 mmHg, 60 to 80 mmHg, 80 to 90 mmHg, 90 mmHg and above
T peak bps (The exercise test's highest systolic blood pressure)	Less than 160 mmHg, 160 to 180 mmHg, 180 mmHg and above
T peak bpd (The activity test's highest diastolic blood pressure)	Less than 75 mmHg, 75 to 80 mmHg, 80 mmHg and above
HTN (elevated blood pressure)	Yes: 1, No: 0
Rest ECG (Resting ECG results)	0: Normal 1: Non-cardiac wave 2: Elevated left ventricular thickness according to Estes criterion
Hexing (Exercise-induced angina)	Yes: 1, No: 0
Theorist (Heart rate at rest)	Less than 60 bpm, 60 to 100 bpm, 100 bpm and above
Halacha (Maximum heart rate)	Less than 148 bpm, 148 bpm and above
Old Peak	Less than 1/8, 1/8 and above
Slope (deviation of the ST segment during exercise testing)	1: Upsloping 2: Flat 3: Down sloping
Thala (Thallium scan)	3: normal 6: fixed defect 7: reversable defect
CA (Major vessels used in fluoroscopy and their numbers)	{0, 1, 2, 3}
Class	Angiographic status 0: Healthy (less than 50% stenosis) 1: Diseased (more than 50% stenosis)

Table 1. Outlining the features of this dataset and the distinct intervals. *To ensure compliance with medical standards and statistical consistency, discretization intervals are specified using normalized data ranges and clinical thresholds (such as American Heart Association guidelines).*

Feature Type	Feature Name	Data Source	Description	Role in Proposed Methodology
Image-Based	Heart Region Area	EchoNet-Dynamic	Figure 6 shows the area of the segmented cardiac region (such as the left ventricle) as determined by the FCN and U-Net models.	utilized as a characteristic that ResNet-50 extracted to examine the structure of the heart and find anomalies in the categorization of cardiac diseases.
Image-Based	Mean Pixel Intensity	EchoNet-Dynamic	Figure 6 displays the average pixel intensity in the cardiac regions that have been segmented following preprocessing (noise reduction and normalization).	identifies illness patterns by indicating changes in intensity, which is then fed into deep learning models for combination with clinical data.
Clinical	Serum Cholesterol (Chol)	Cleveland UCI	Level of serum cholesterol (mg/dL), discretely normalized in the ranges [200, 239], (239, +∞), and (-∞, 200).	In order to predict heart illness, a crucial clinical feature is combined with image-based features in SVM and MLP models.
Clinical	Resting Systolic Blood Pressure (T rest BPs)	Cleveland UCI	Systolic blood pressure (mmHg) at rest is normalized to the ranges (-∞,90), [90,120], (120,140], (140,+∞).	To improve diagnostic accuracy, the multimodal design combines a clinical risk factor with characteristics retrieved from images.

Table 2. Comparison of features based on images in the suggested approach to heart disease diagnosis.

Univariate outlier data

In univariate outlier analysis, outliers are detected based solely on the box plot, without regard to additional variables. A box plot is a graphical representation that illustrates variations in a single variable. This graph is derived from the statistical metrics of the minimum value, the first quartile (Q1), the median (Q2), the third quartile (Q3), and the maximum value.

The graph in Fig. 5 illustrates the distance between the first and third quartiles, as well as the median, or second quartile, of the box plot. According to Eq. (4), the IQR value is computed, whereas Eqs. (5) and (6) establish the top and bottom boundaries of the graph.

$$IQR = Q3 - Q1 \tag{4}$$

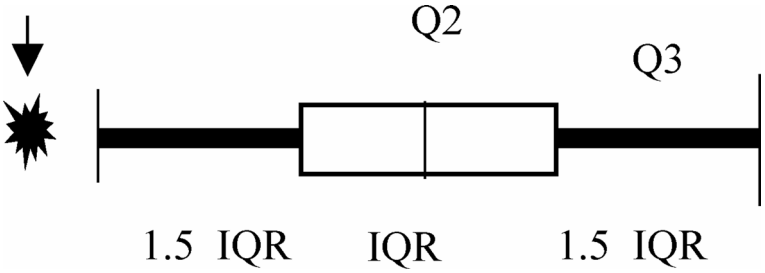

Fig. 5. Distance between the first and third quartiles.

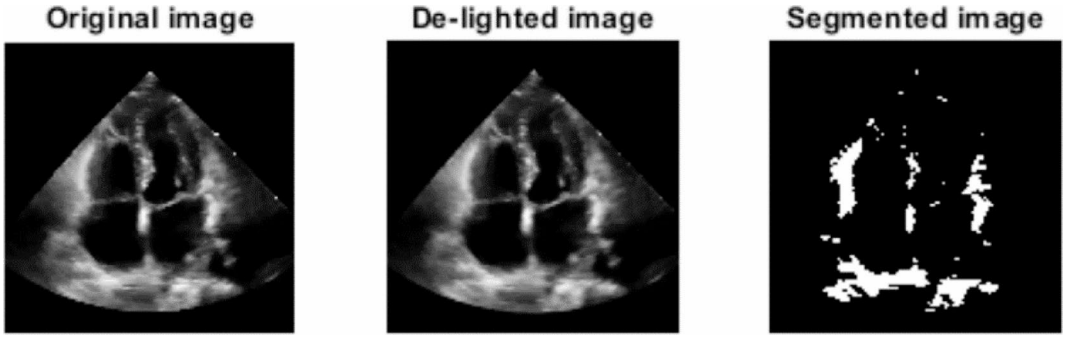

Fig. 6. A cardiac ultrasound image's segmentation steps include the raw data, the preprocessed image, and the segmented image.

$$Lower\ limit:\ Q1 - (1.5 * IQR) \tag{5}$$

$$Upper\ limit:\ Q3 + (1.5 * IQR) \tag{6}$$

Data that exceeds the upper limit or falls below the lower limit is classified as outlier data[49]. Considering that certain qualities are medical in nature, the strategy for transforming outlier data into normative data stipulates that if the data falls within a medical range and pertains to the patient class, it remains unaltered. It serves as a risk factor for heart disease and contributes to the development of a more precise model; however, if the individual falls within the healthy category, the outliers will adjust to the nearest normal range. This study initially identifies and addresses univariate outliers for each characteristic, followed by the identification and management of multivariate outliers as outlined in Sect. 4.2.2. The input and output data of the preprocessing and segmentation procedure in the suggested method are illustrated in Fig. 2, which displays a raw and segmented cardiac ultrasound image. The segmented image (right) is the outcome of utilizing FCN and U-Net models to separate important cardiac regions, whereas the raw image (left) serves as the starting data for applying noise removal and normalization procedures. The significance of preprocessing in enhancing image quality and obtaining precise features for deep learning models is illustrated in this figure. Lastly, the suggested multimodal architecture uses this figure as a foundation for combining clinical and imaging data.

Three visual phases for segmenting a cardiac ultrasound image are depicted in Fig. 6. Three images make up the figure: The raw cardiac ultrasound data, including the first features and noisy heart structures, is displayed in the first image. The second image demonstrates the outcome of preprocessing techniques that enhance image quality and highlight important cardiac regions, such as leveling pixel intensity to the interval [0,1] and denoising using a Gaussian filter. Important parts of the heart, including the left ventricle, are precisely isolated from the background and ready for the extraction of significant features in the third image, which displays the final segmentation output using deep learning models like FCN and U-Net.

Figure 7 illustrates the box plot of the cholesterol variable. Considering that this feature has a medical threshold and the outliers reside within the upper range, these data points for ill individuals are deemed a risk factor and will remain unchanged. Conversely, the four outlier data points for healthy individuals will be adjusted to their nearest permissible values, specifically the upper and lower limits.

Figure 8 depicts the architecture of a hybrid system for diagnosing heart disease, incorporating clinical data, medical imaging, and sensor data. Data is gathered from various sources in the initial layer, including clinical records (such as medical history, blood tests, and demographic details), medical images (such as echocardiography, cardiac MRI, CT scans, and chest X-rays), and sensor data (such as heart rate, blood pressure, and oxygen saturation levels). In the second layer, pertinent features are derived from these data sources; medical images are scrutinized using image processing methodologies and convolutional neural networks (CNNs) to extract essential features, whereas clinical and sensor data are evaluated through signal analysis and quantitative

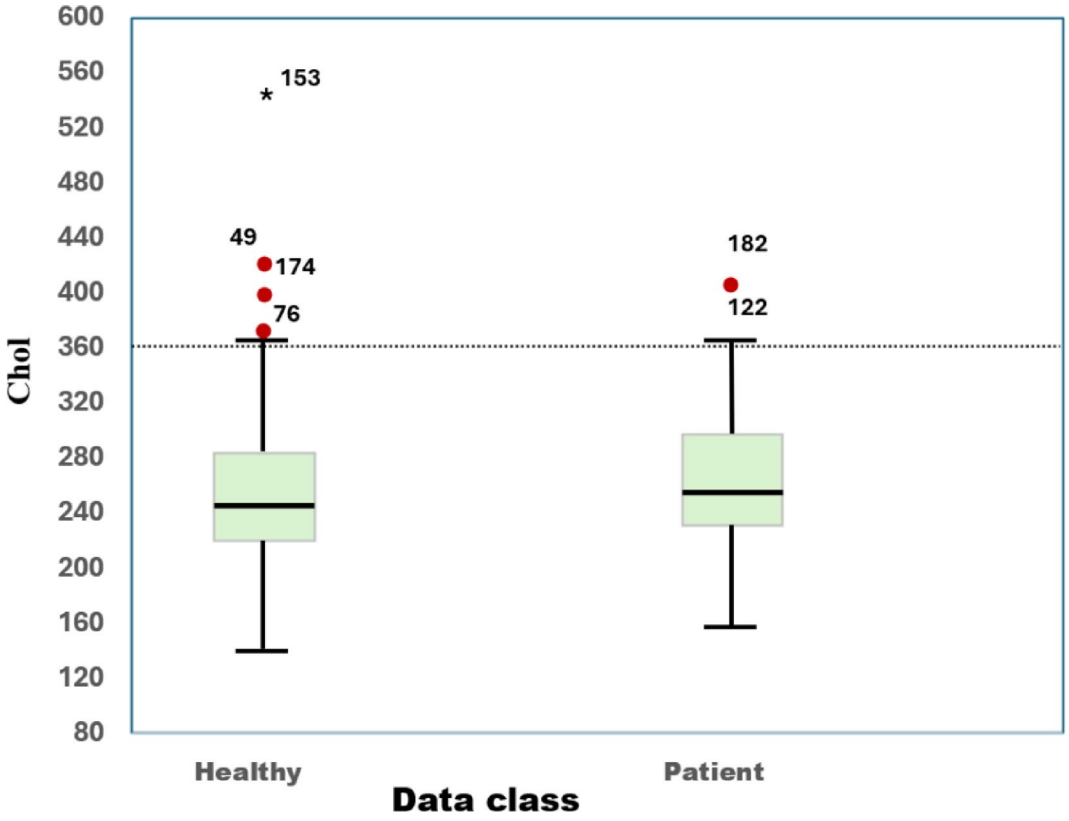

Fig. 7. Boxplot of cholesterol using univariate outlier data.

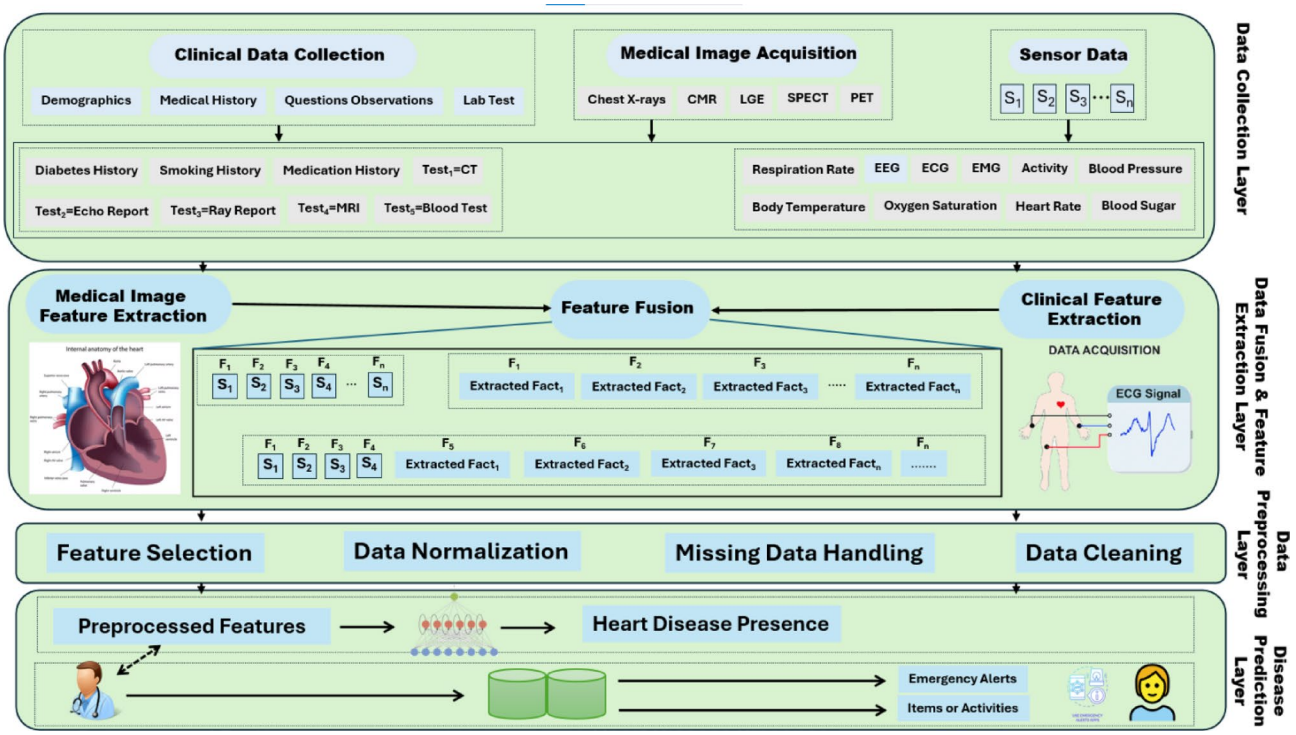

Fig. 8. Proposed architecture of a hybrid system for heart disease diagnosis.

feature extraction. The collected characteristics are subsequently integrated into a cohesive dataset for additional processing.

In the subsequent layer, the data undergoes preprocessing procedures including feature selection, normalization, management of missing data, and data cleansing to enhance quality and consistency. Subsequent to preprocessing, the enhanced features are input into machine learning models and deep neural networks to forecast the probability of heart disease in patients. These models, such as SVM, Random Forest, XGBoost, and deep neural networks, concurrently evaluate both imaging and clinical data to improve diagnostic precision. Ultimately, the system's output may encompass disease predictions, emergency alarms, and treatment recommendations for both physicians and patients, therefore enhancing the accuracy, speed, and non-invasive characteristics of heart disease diagnosis.

Data on multivariate outliers

To detect multivariate outliers in the dataset, the dependent variable is the data class, while the independent variables are a collection of numerical properties. Subsequently, the Mahalanobis distance of the data is computed in relation to the class, and outliers are found and eliminated from the dataset using boxplots and histograms. The Mahalanobis distance, utilizing the data covariance matrix, quantifies the distance of each observation in multidimensional space from the mean center of all observations. Consequently, it may serve as an appropriate metric for identifying multivariate outliers. Figure 9 illustrates a box plot depicting the Mahalanobis distance of the data in relation to the class.

As stated in Sect. 4.2.1, subsequent to analyzing the outliers for each feature, the total multivariate outliers were assessed. A total of 8 data points (8 sick or healthy persons) were detected as multivariate outliers throughout the processing of stages 1, 2, and 3, and subsequently removed. Figure 9 illustrates the extent of data dispersion according to the Mahalanobis interval pertaining to the class[44]. The Mahalanobis interval for each dataset is computed utilizing Eq. (7).

$$Mi^2 = (X_i - \mu_{\,i})^T C^{-1} (X_i - \mu_{\,i}) \tag{7}$$

M^2 represents the Mahalanobis distance of data i, X_i denotes the vector of variables for the i-th sample, and μ signifies the vector of mean values of independent variables. In this context, C represents the covariance matrix of the training data (independent variables), whereas T denotes the transposition of the expression within the parenthesis. Mahalanobis distance resembles Euclidean distance, however it is adjusted by the covariance matrix. Figure 10 illustrates that data points with a Mahalanobis distance exceeding 54.5% in relation to the class are classified as outliers and subsequently excluded from the dataset.

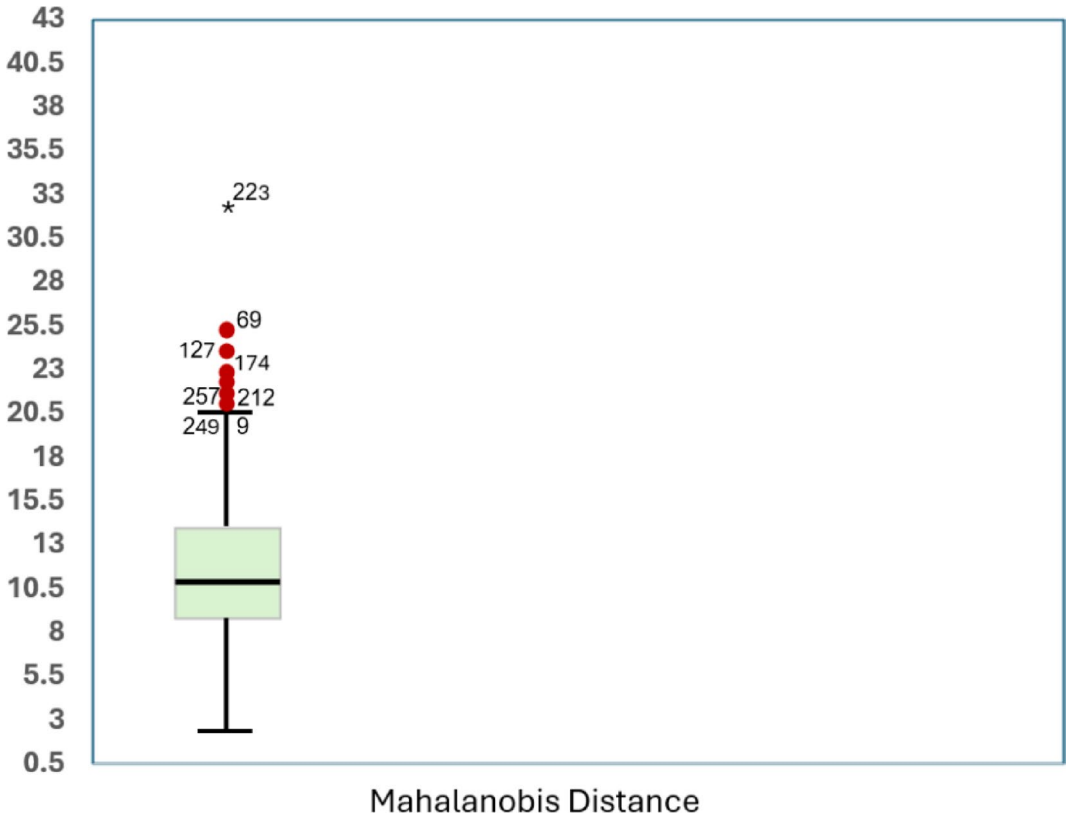

Fig. 9. Mahalanobis distance box plot of data for multivariate outlier detection.

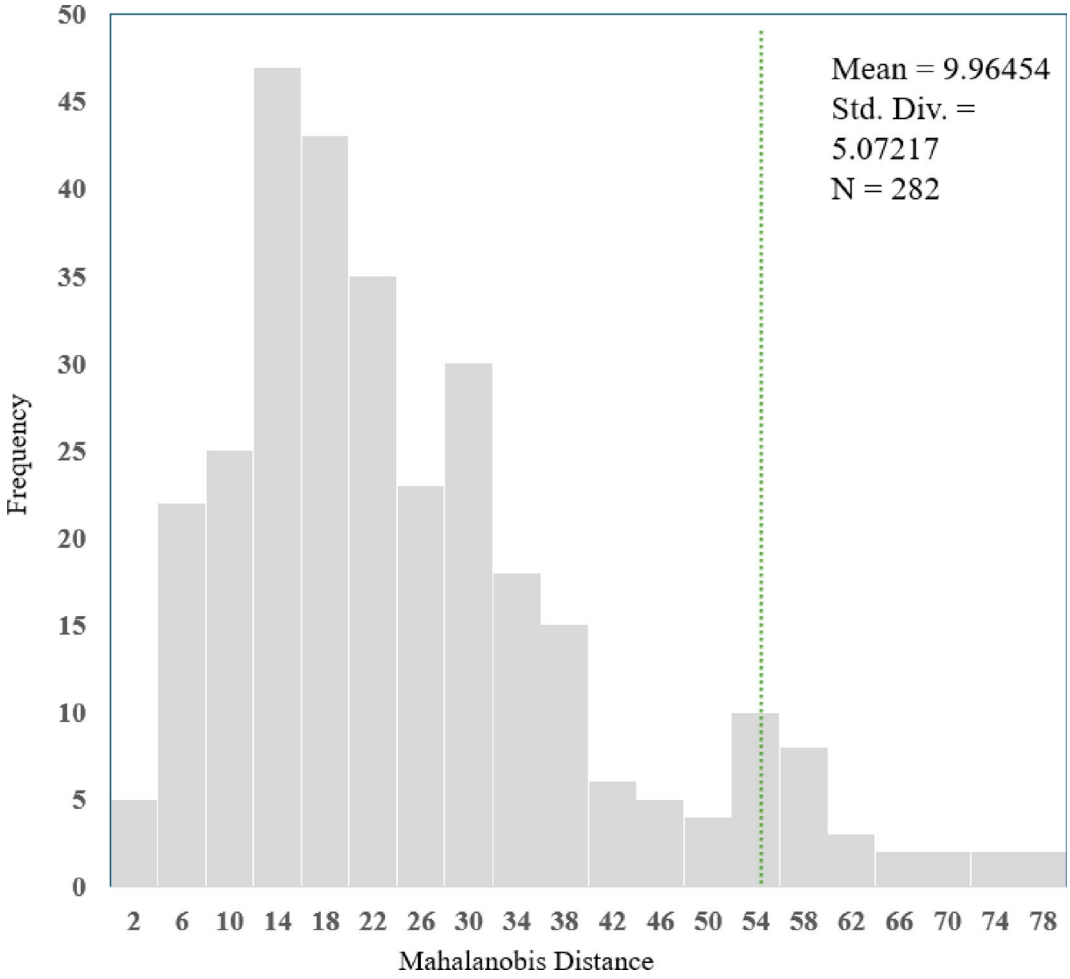

Fig. 10. Data dispersion according to Mahalanobis distance in relation to data class.

Figure 10 shows how the dataset's multivariate outliers are discovered using Mahalanobis distance from the class variable (healthy or diseased). The scatter plot shows each Cleveland Clinic Heart Patient Dataset sample against its estimated Mahalanobis distance, a metric that evaluates the distance of a data point from the distribution mean, corrected by the covariance matrix. The x-axis may be an index or feature dimension, while the y-axis shows Mahalanobis distance values with a threshold line (about 54.5%) separating typical data points from outliers. Multivariate outliers are points above this threshold that deviate significantly from their class distribution.

Numerical data normalization

Data normalization is a data scaling technique utilized in machine learning algorithms, applicable to numerical features for several objectives. In health research, the challenges of data access, security, and individual privacy can be partially addressed through data normalization. Normalization is crucial in the modeling process and model efficacy, significantly influencing the learning velocity of the model. It is predominantly utilized in scenarios where the data ranges vary, aiming to mitigate the adverse effects of disparate numerical ranges on model performance. This study employed the MIN-MAX normalization technique to standardize numerical data. The dataset for each feature has been normalized to a range between the New_{max} and New_{min}, specifically 1 and 0, in accordance with Eq. 8.

$$X_i = New_{min} + (New_{max} - New_{min}) * \frac{X_i - X_{min}}{X_{max} - X_{min}} \tag{8}$$

Where X_{min} is the minimum value of the data before normalization, X_{max} is the maximum value of the data before normalization, New_{min} is the minimum value after normalization, and New_{max} is the maximum value after normalization. X_i is also mapped to a value in the range New_{min} and New_{max}.

Numerical data discretization

Owing to the characteristics of certain modeling techniques employed in this study, the numerical features must be discrete and transformed into suitable intervals. Given that certain aspects have a medical domain;

the discretization flowchart has been implemented as shown in Fig. 10. The outcomes of the discretization are presented in Table 1.

The detailed procedure for evaluating and diagnosing cardiac disease utilizing a combination of EchoNet and Cleveland UCI data is depicted in the flowchart in Fig. 11 First, 512-dimensional ResNet-50 is used to extract clinical data and characteristics from EchoNet pictures from Cleveland UCI. Following denoising, normalization, and EchoNet-specific segmentation in the preprocessing phase, ResNet-50 is used to extract the features. Following feature selection, these features go through the extraction process after being concatenated with UCI data. If medically verified, discretization based on the medical domain is carried out by looking at the association with class features; if not, sampling-based clustering is used. This phase is carried out if discretization optimization is feasible; if not, discretization is carried out using the density of equal intervals. Lastly, two categories of present/absent cardiac disease are classified using ADA Boost/SVM algorithms, and performance measures including accuracy and AUC are presented.

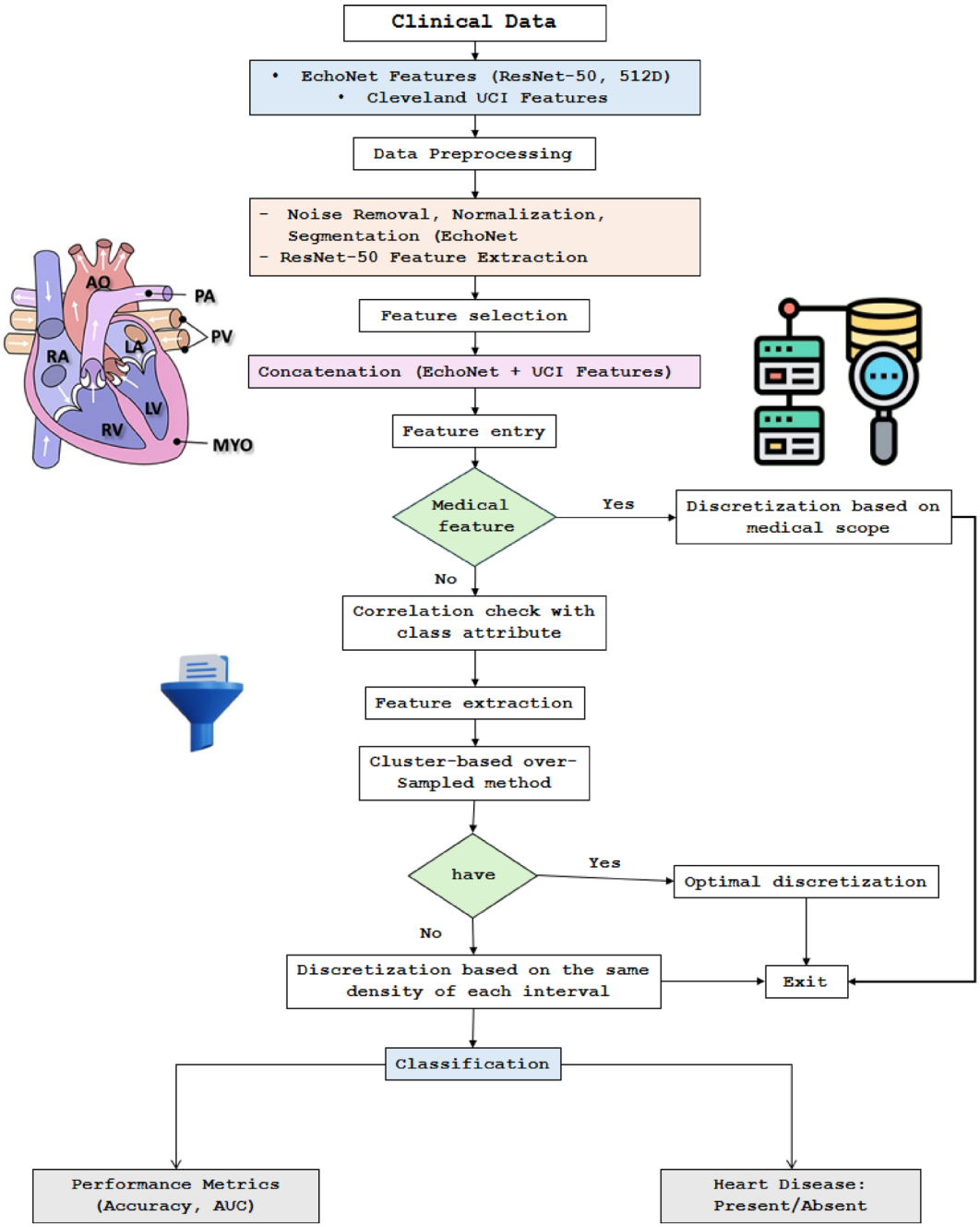

Fig. 11. Flowchart showing the discretization of numerical data for the diagnosis of heart disease.

Experimental results

This section delineates the results of the proposed hybrid methodology for diagnosing heart illness, assessed through comprehensive experiments utilizing the Cleveland Clinic Heart Patient Dataset from the UCI repository. The execution was conducted in a high-performance computing environment using an Intel Core i7-9700 K processor, 32 GB of RAM, and an NVIDIA GeForce RTX 2080 Ti GPU to accommodate the computational requirements of deep learning models and image processing activities. The software configuration utilized Python 3.9 as the principal programming language, incorporating libraries including TensorFlow 2.6, PyTorch 1.10, Scikit-learn 1.0, and OpenCV 4.5 for model construction, training, and image analysis. Furthermore, SPSS Statistics and RapidMiner were utilized in the data preprocessing phase to guarantee rigorous statistical analysis and feature engineering. A critical aspect of the modeling process is feature selection and comprehending the association among features. Figure 12 illustrates the correlation coefficients of several significant features within this dataset.

The features Thala, Hexing, Old Peak, Halacha, and CP have the strongest association with the data class. The correlation between two features, $x\ and\ y$, is computed based on the connection outlined in (9). In this context, Corer denotes the correlation between two features, Cove represents the covariance of two features, ρ signifies the standard deviation, E indicates the arithmetic expectation, and μ refers to the mean of a feature.

$$Corr\,(x,y) = \frac{cov(x,y)}{\rho_{\,x}\rho_{\,y}} = \frac{E[(x-\mu_{\,x})\times\ \left(y-\mu_{\,y}\right)]}{\rho_{\,X}\rho_{\,y}} \tag{9}$$

The correlation coefficient ranges from −1 to 1 and signifies both the strength and nature of the association between two variables (direct or inverse). If two features are unrelated, the correlation will equal 0. Another criterion for evaluating features is the Pearson chi-square test, which assesses the score of each feature in relation to the class feature. This test is computed using Eq. (11), where X^2 represents the test result, O denotes the observed frequencies, and E signifies the predicted frequencies. This test is suitable for nominal variables and primarily serves to assess the importance of the disparity between observed and expected frequencies, which was utilized in this study for a discrete data set.

$$X^2 = \sum_{k=1}^{n} \frac{(o_k - E_k)}{E_k} \tag{10}$$

The existence of a feature exhibiting a strong correlation or score in relation to the data class during modeling does not invariably enhance model performance; nonetheless, it does elevate the likelihood of increasing model efficiency. Figure 13 illustrates the scores of each feature as determined by the Pearson Chi-square test. The

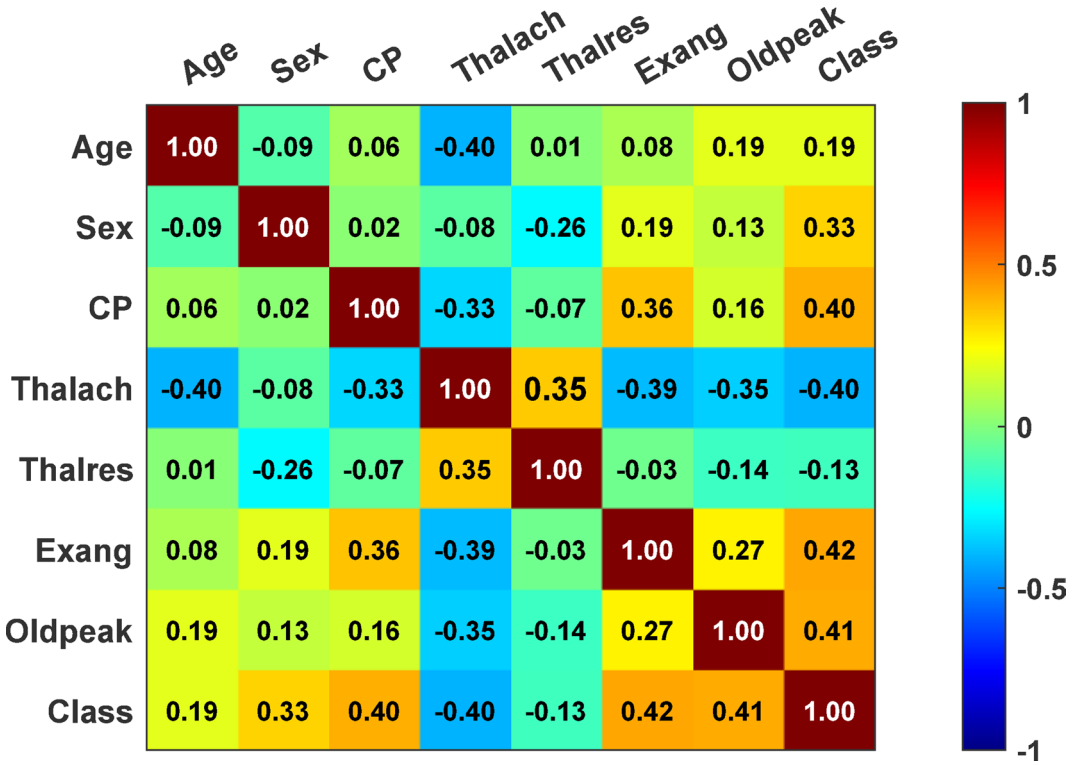

Fig. 12. Displaying the correlation of features.

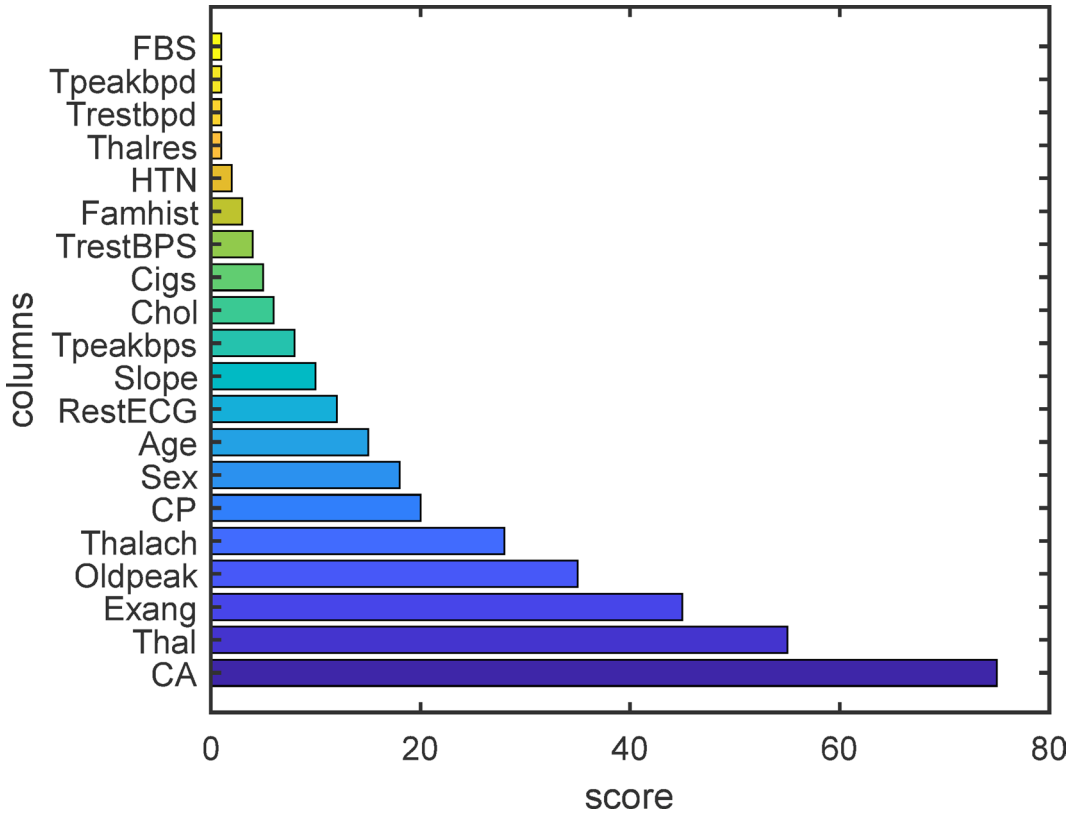

Fig. 13. Pearson Chi-square test ranking of each attribute in relation to the class.

findings from this test align with those derived from the correlation criterion in Fig. 12. Figure 14 illustrates the distribution of healthy and ill individuals by gender across various age groups. The picture indicates that males get heart disease at an earlier age than women, and as illustrated in Fig. 15, the probability of having heart disease escalates with age for both genders.

Figure 15 illustrates that the Old peak characteristic for ill persons typically exceeded 1.8, and during the discretization phase, this characteristic was categorized into values below and above 1.8. Figure 16 illustrates the cumulative sum of variance rates as a function of the number of PCA components. It is evident that utilizing 10 to 15 PCA components was suitable for dimensionality reduction; hence, this same quantity was employed during the modeling phase with PCA components.

In summary, Fig. 16 illustrates that the data preparation phase precedes the modeling phase. This phase encompasses a series of procedures that adequately prepare the data for the modeling phase. To enhance the efficacy of modeling algorithms and identify superior input parameters (such as determining the optimal number of input features, selecting the appropriate number of components, and establishing optimal discrete intervals for numerical features), data visualization and feature selection techniques have been employed. Additionally, the measures implemented during the data preparation phase are designed to enhance the efficacy of predictive models for cardiovascular illnesses. The subsequent section delineates the modeling and implementation process.

A thorough comparison between clinical factors from the Cleveland UCI dataset and characteristics taken from echocardiographic imaging data from the EchoNet-Dynamic dataset is shown in Table 3. Using a U-Net-based segmentation model and an approximate scale of 0.1 mm per pixel, imaging features were computed, including the approximate size of important cardiac regions such as the left ventricle, right ventricle, left atrium, right atrium, and a substructure. These characteristics were combined with clinical information taken from the distinct areas in Table 1, including systolic and diastolic blood pressure and cholesterol levels.

Modeling and implementation phase

This section presents the machine learning techniques Decision Tree, Random Forest, XGBoost, and Support Vector Machine, which were employed for modeling. The modeling was subsequently conducted using multilayer perceptron neural networks. A singular data set was utilized to train all machine learning algorithms, and 20% of the data served as a unified test data set for comparative analysis of the algorithms' findings. The algorithms were initially evaluated from the normalized discrete features, followed by the components derived from the PCA technique, on the test data for both scenarios, as presented in Tables 4 and 6. Additionally, to acquire parameters approximating the optimal for machine learning algorithms, random search utilizing cross-validation and, for neural networks, the MLP Talus Scan method for network search was employed. The assessment of the models is conducted utilizing relations (12) to (15). The support vector machine algorithm achieves the best accuracy

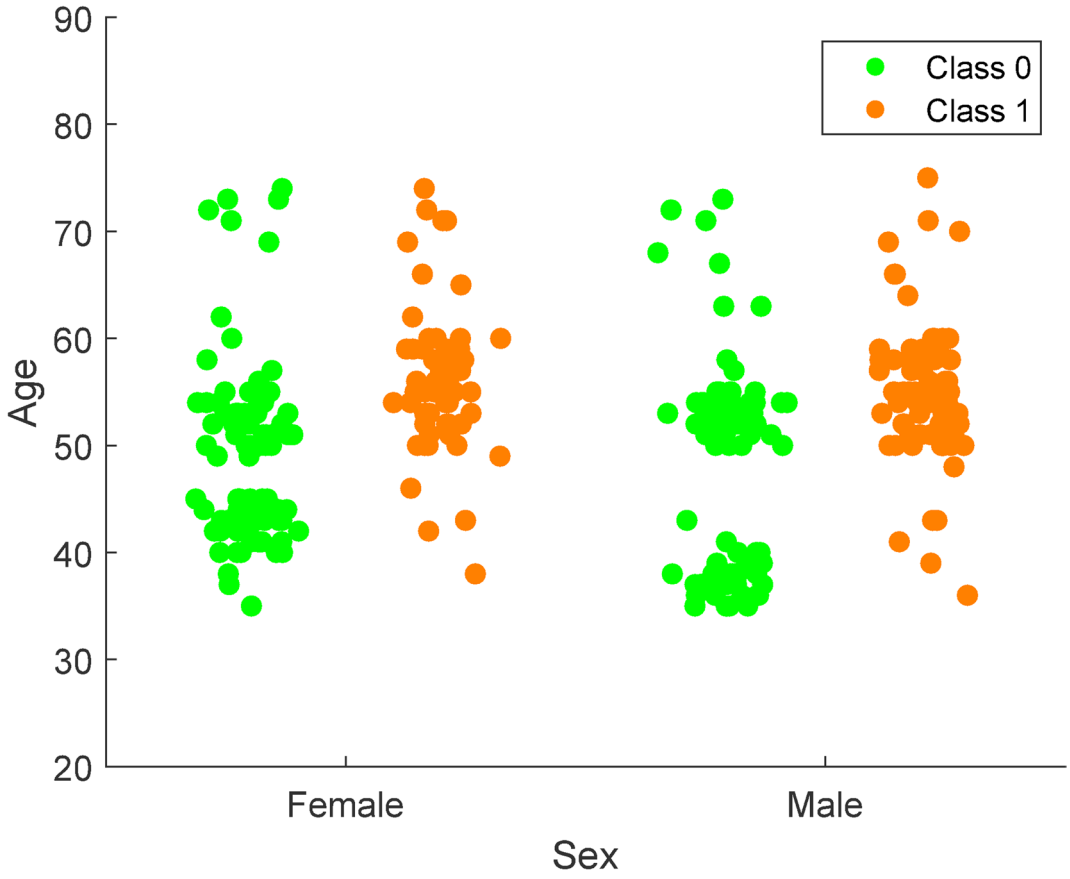

Fig. 14. Shows the frequency of both healthy and ill individuals by gender at various ages (0: women and the healthy class, and 1: men and the sick class).

among machine learning algorithms at 92.9%, while the multilayer perceptron neural network attains the most accuracy among neural networks at 94.6%.

$$Accuracy = \frac{TP + TN}{TP + EN + FP + TN} \tag{11}$$

$$Precision = \frac{TP}{TP + FP} \tag{12}$$

$$Recall = \frac{TP}{TP + FN} \tag{13}$$

$$F1 - Score = \frac{2\,Precicion * Recall}{Precicion + Recall} \tag{14}$$

Where TP, TN, FP and FN are predicted (true positive class), correct prediction (true negative class), incorrect prediction (true negative class), incorrect prediction (true class) and incorrect prediction (true class). Equation (14) is with harmonic measures of accuracy and recall[40]. In Table 4D1 is the dataset with discrete features or software D2 is the dataset, the features generated by the original model are analyzed. Also, DT represents the decision tree algorithm, RF represents the random forest algorithm, XG represents the XG Boost algorithm and SVM represents the support vector machine algorithm. Also, all the results in Tables 4 and 6 are calculated in terms of percentage. According to Table 4, the highest accuracy rate among machine learning algorithms is related to the support vector machine algorithm and is 92.9%.

To enhance outcomes and augment modeling accuracy, multilayer perceptron neural networks have been employed. A significant issue related to neural networks is model overfitting inside these networks. The developed model must ensure that minimizing the training data error does not elevate the test data error, necessitating precise adjustments to the network's stopping time and the amount of parameters for each network.

To ascertain the optimal number of iterations, 15% of the training dataset was designated as evaluation data. Utilizing a multilayer perceptron neural network, the errors for both the training and evaluation datasets were computed, thereby establishing the suitable number of iterations to terminate the training algorithm. Typically, in neural networks, as the number of training iterations increases, the errors for both training and evaluation datasets diminish; however, this is true only until the errors for both datasets drop over training time steps.

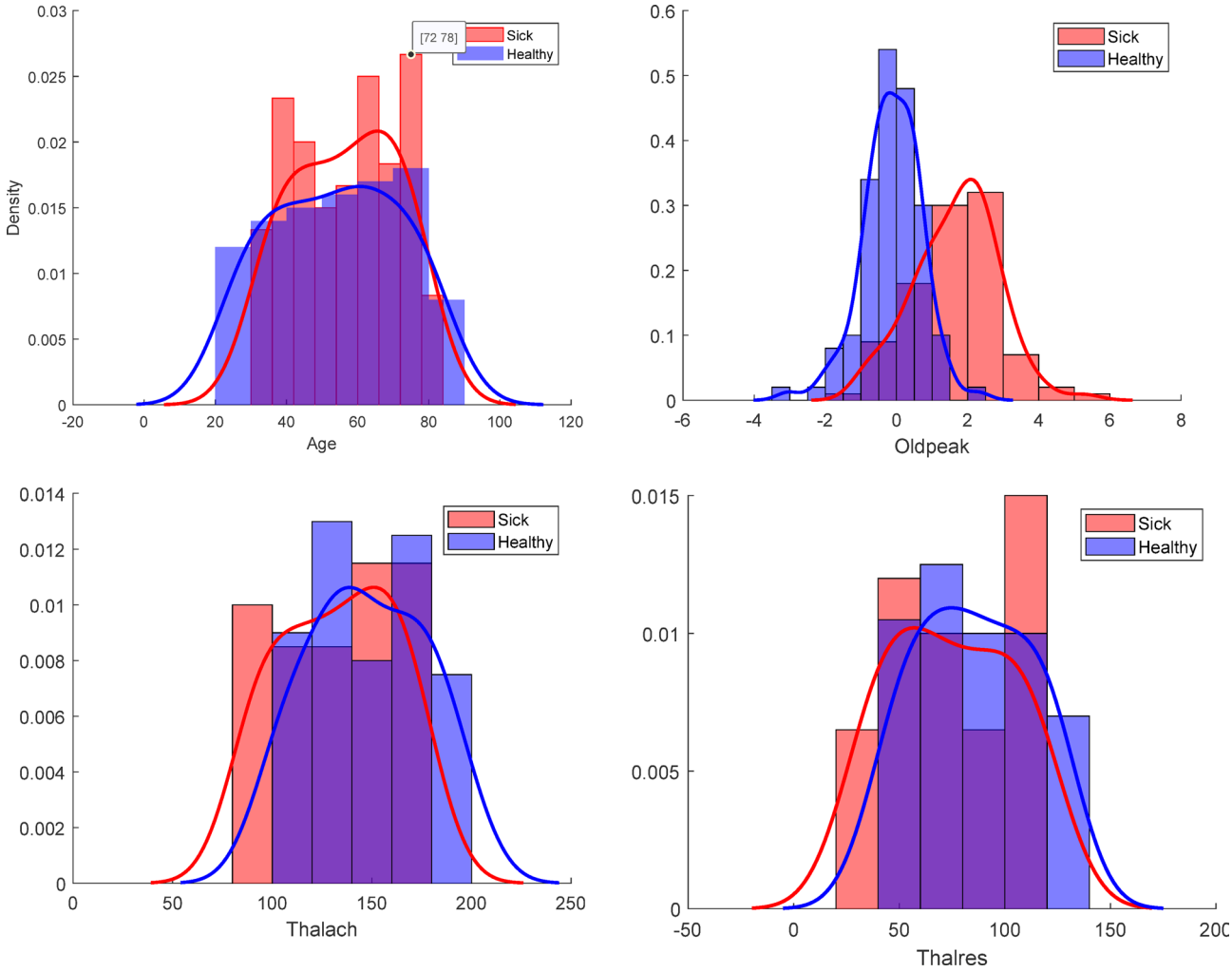

Fig. 15. Frequency distribution of Thalach, Thalres, Age, Old peak features based on data class.

When the training data error diminishes but the evaluation data error escalates, the training procedure ought to be terminated (Fig. 17). It is noted that between 45- and 50-time steps (repeat), both the training error and evaluation error diminish; however, beyond this range, while the training error continues to decline, the evaluation error escalates, indicating that the training procedure should be terminated. Moreover, alongside the iterative steps, the network architecture is highly effective in mitigating model overfitting; thus, the selection of layers and neurons per layer must ensure that an increase in network parameters does not compromise the network's performance on test data. Table 5 illustrates the construction of MLP neural networks. Furthermore, Table 6 presents the outcomes derived from MLP neural networks applied to the test data.

Table 6 indicates that the multilayer perceptron neural network, trained on normalized data, achievd the maximum accuracy of 94.6%. The best outcomes from the different machine learning algorithms and artificial neural networks (ANN) used in this study are displayed in Fig. 18. These include two Keras-based models (XG and ANN-Keras), Support Vector Machine (SVM), Random Forest (RF), Multilayer Perceptron (MLP), and Decision Tree (DT).

Comparative analysis of the proposed method with existing studies

Table 7 summarizes the optimal results from the models developed in this work with the findings from the existing literature, clearly demonstrating the enhancement in heart disease prediction modeling using UCI cardiac data in this research. It is important to highlight that all research referenced in Table 7 utilized UCI heart data, and in this study, 20% of the data was randomly picked for the evaluation of all models. Due to the unavailability of test data from the comparative studies, certain samples from this study's test data may differ from those of another research. It is important to note that during the data processing and symbolization phases, both the Python programming language and the tools SPSS Statistics and RapidMiner1 were utilized, while the modeling section exclusively employed Python to develop various predictive models for heart disease.

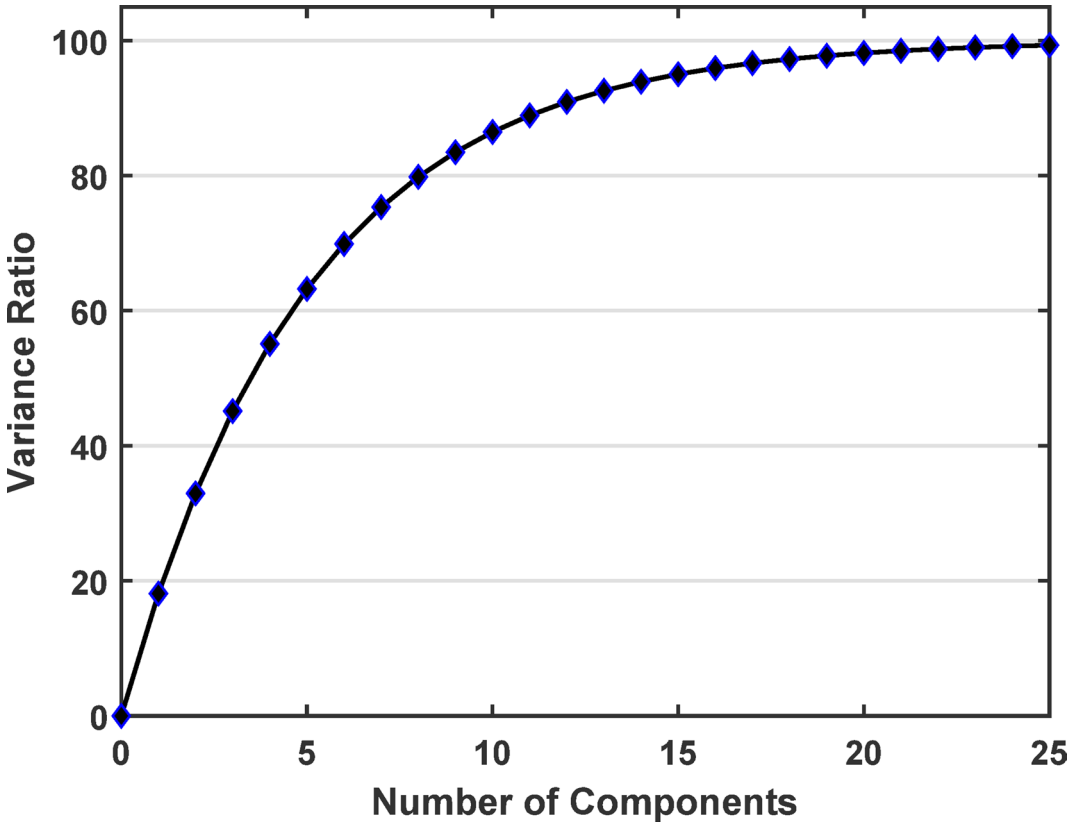

Fig. 16. Variance rate cumulatively depends on the number of PCA components.

Feature Type	Feature Name	Value Range/Size	Data Source	Description
Imaging	Left Ventricle Diameter (LV)	28 mm	EchoNet	Segmented region shown in red
Imaging	Right Ventricle Diameter (RV)	22 mm	EchoNet	Segmented region shown in green
Imaging	Left Atrium Diameter (LA)	25 mm	EchoNet	Segmented region shown in yellow
Imaging	Right Atrium Diameter (RA)	20 mm	EchoNet	Segmented region shown in blue
Imaging	Secondary Cardiac Structure	8 mm	EchoNet	Segmented region shown in pink/purple
Clinical	Serum Cholesterol (mg/dL)	[200, 239]	Cleveland (UCI)	Measured blood cholesterol level
Clinical	Systolic Blood Pressure (mmHg)	[90, 120]	Cleveland (UCI)	Resting systolic pressure
Clinical	Diastolic Blood Pressure (mmHg)	[60, 80]	Cleveland (UCI)	Resting diastolic pressure

Table 3. A comparison between clinical factors from the Cleveland UCI dataset and imaging features from EchoNet-Dynamic based on image data representation.

Algorithm	Data	Accuracy (%)	Precision (%)	Recall (%)	F1 – Score (%)
DT	D1	87.5	88.1	86.1	86.8
DT	D2	89.3	90.6	87.6	88.6
RF	D1	91.1	90.6	91.1	90.8
RF	D2	85.7	85.2	85.2	85.2
XG	D1	91.1	91	90.4	90.7
XG	D2	87.5	87.3	86.8	87
SVM	D1	92.9	93.3	92	92.5
SVM	D2	92.9	93.3	92	92.5

Table 4. Results of models built using decision tree, random forest, XG boost and support vector machine algorithms on test data.

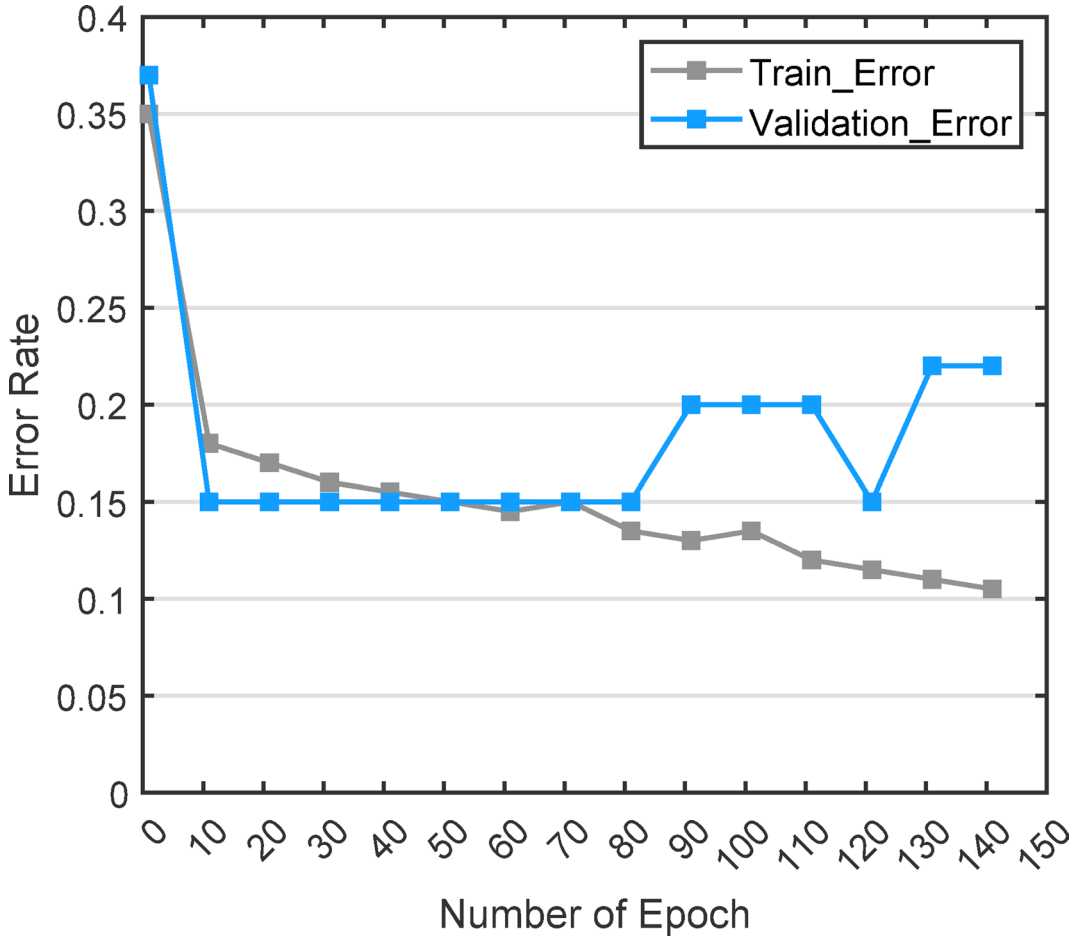

Fig. 17. Error comparison between training and evaluation data throughout iterations.

Network	Number of Hidden Layers	Number of Neurons in Layers	Activation Functions
MLP	One Hidden Layer	Hidden Layer: 10, Output Layer: 1	Hidden Layer: ReLU Output Layer: Sigmoid
MLP	Two Hidden Layers	First Hidden Layer: 12 s Hidden Layer: 8 Output Layer: 2	Hidden Layers: ReLU Output Layer: Softmax

Table 5. MLP neural network architecture used in this research.

Neural Network	Data	Accuracy (%)	Precision (%)	Recall (%)	F1 Score (%)
MLP (One Hidden Layer)	D1	94.6	94.8	94.1	94.4
MLP (One Hidden Layer)	D2	87.23	87.3	86.8	87.0
MLP (Two Hidden Layers)	D1	91.1	93.4	89.1	90.3
MLP (Two Hidden Layers)	D2	89.3	88.9	88.9	88.9

Table 6. Findings from test data using MLP neural networks.

Conclusion

This study emphasizes the significance of early cardiac disease diagnosis by developing predictive models utilizing various machine learning methods and neural networks. This study's proposed method acknowledges that prediction models can achieve satisfactory performance when data is optimally processed and modeled. Consequently, multiple data processing techniques have been employed, tailoring the data preparation to each specific modeling algorithm. Consequently, as outlined in Sect. 2.3 of this study, the dataset was converted into two formats: normalized data and discrete data. Furthermore, normalized discrete data was utilized once for model construction, while features generated by the principal component analysis approach were employed twice. The classification accuracy of the decision tree technique was enhanced by utilizing principle components

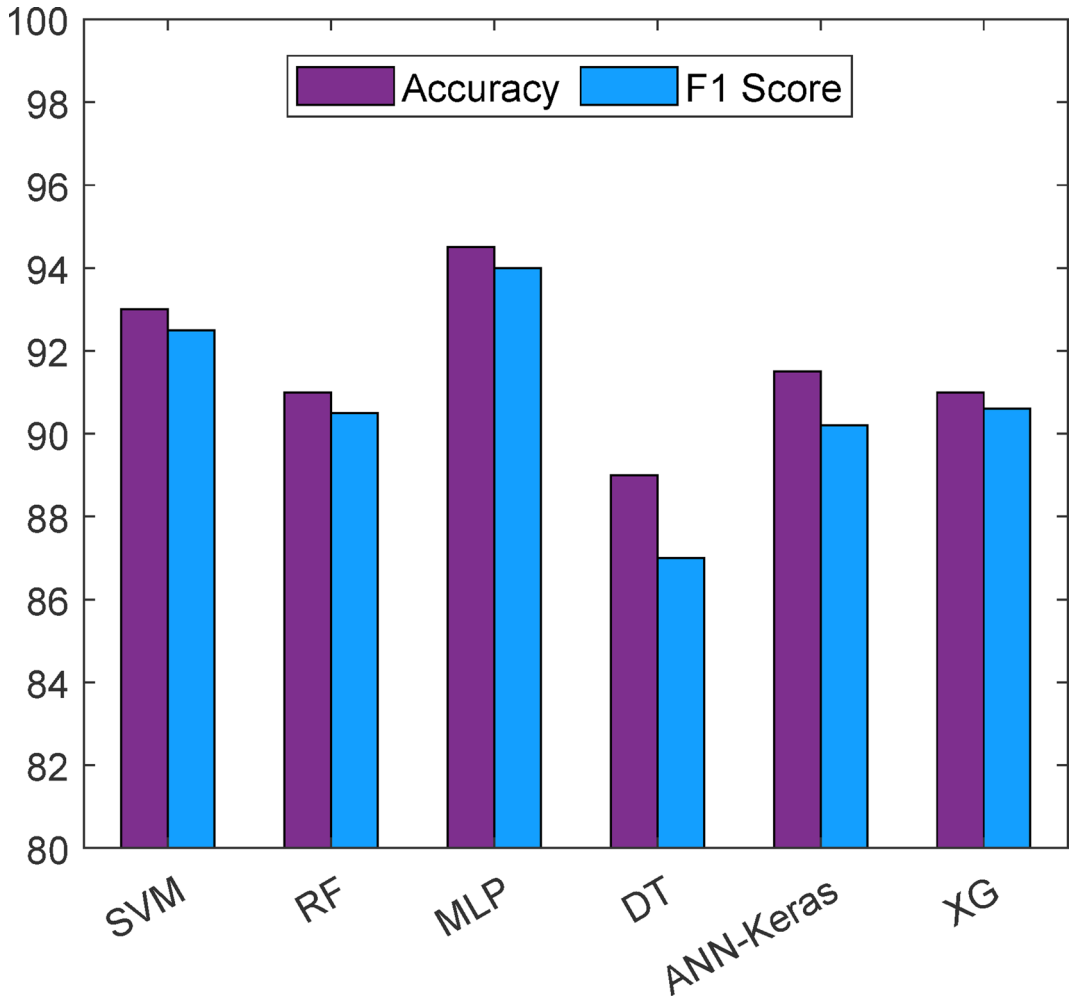

Fig. 18. The best results obtained from all algorithms used in the research.

	Research	Best Accuracy (%)
1	This Work	96
2	[8]	85.03
3	[22]	82.91
4	[41]	83.33
5	[47]	87.37

Table 7. Contrasting the best findings from this study with those from earlier studies.

rather than discrete features. Ultimately, diverse modeling algorithms were employed to develop predictive models for cardiovascular illnesses, considering parameter optimization. The support vector machine algorithm exhibits the best accuracy among machine learning methods, with 92.9%. In another segment of this research, the MLP neural network was employed to enhance the precision of disease prediction models, achieving the greatest accuracy of 96% using a single hidden layer. In this network configuration, each increase in parameters necessitates a sufficiently large dataset; thus, employing a hidden layer with 10 neurons yields the highest accuracy of 94.6%. It is crucial to acknowledge that identifying the appropriate parameters for each neural network is a complex and critical endeavor. Consequently, an online search employing the Scan Talos methodology was conducted. Ultimately, it is noteworthy that the study indicates a direct correlation between heart disease and age, with the risk of heart disease escalating as individuals age. The onset age of heart disease in men is earlier than in women, with women experiencing heart disease at older ages. The characteristics of Ex ang, Old peak, CP, CA, Thal, and Thalach are critical in predicting and developing heart disease symptoms.

Data availability

The datasets used and/or analyzed during the current study available from the corresponding author on reasonable request.

Received: 9 April 2025; Accepted: 14 July 2025
Published online: 19 July 2025

References

1. Suganyadevi, S., Seethalakshmi, V. & Balasamy, K. A review on deep learning in medical image analysis. *Int. J. Multimedia Inform. Retr.* **11** (1), 19–38 (2022).
2. Ahsan, M. M. & Siddique, Z. Machine learning-based heart disease diagnosis: A systematic literature review. *Artif. Intell. Med.***128**, 102289 (2022).
3. Wang, J., Wang, S. & Zhang, Y. Deep learning on medical image analysis. *CAAI Trans. Intell. Technol.* **10** (1), 1–35 (2025).
4. Hu, F., Yang, H., Qiu, L., Wei, S., Hu, H.,... Zhou, H. Spatial structure and organization of the medical device industry urban network in China: evidence from Specialized, Refined, Distinctive, and Innovative firms. *Front. Public Health*, **13**, 1518327 https://doi.org/10.3389/fpubh.2025.1518327 (2025).
5. Li, H. et al. An algorithm for cardiac disease detection based on the magnetic resonance imaging. *Sci. Rep.***15**(1), 4053 (2025).
6. Kumar, Y., Koul, A., Singla, R. & Ijaz, M. F. Artificial intelligence in disease diagnosis: A systematic literature review, synthesizing framework and future research agenda. *J. Ambient Intell. Humaniz. Comput.***14**(7), 8459–8486 (2023).
7. Alkayyali, Z. K., Idris, S. A. B. & Abu-Naser, S. S. A systematic literature review of deep and machine learning algorithms in cardiovascular diseases diagnosis. *J. Theor. Appl. Inf. Technol.***101**(4), 1353–1365 (2023).
8. Chen, X. et al. Recent advances and clinical applications of deep learning in medical image analysis. *Med. Image. Anal.* **79**, 102444 (2022).
9. Reddy, G. T. et al. Hybrid genetic algorithm and a fuzzy logic classifier for heart disease diagnosis. *Evol. Intell.***13**, 185–196 (2020).
10. Xie, H. et al. Associations of cardiac biomarkers with chronic kidney disease and mortality in US individuals without prevalent cardiovascular disease. *Sci. Rep.***15**(1), 15001 (2025).
11. Cai, L., Gao, J. & Zhao, D. A review of the application of deep learning in medical image classification and segmentation. *Annals Translational Med.* **8** (11), 713 (2020).
12. Haq, A. U., Li, J. P., Memon, M. H., Nazir, S. & Sun, R. A hybrid intelligent system framework for the prediction of heart disease using machine learning algorithms. *Mob. Inform. Syst.* **2018** (1), 3860146 (2018).
13. Wu, Q. et al. A novel onco-cardiological mouse model of lung cancer-induced cardiac dysfunction and its application in identifying potential roles of tRNA-derived small RNAs. *Biomed. Pharmacother.***165**, 115117. https://doi.org/10.1016/j.biopha.2023.115117 (2023).
14. Chen, L. et al. HPDA/Zn as a CREB inhibitor for ultrasound imaging and stabilization of atherosclerosis plaque. *Chin. J. Chem.***41**(2), 199–206. https://doi.org/10.1002/cjoc.202200406 (2023).
15. Shukur, B. S. & Mijwil, M. M. Involving machine learning techniques in heart disease diagnosis: A performance analysis. *International Journal of Electrical and Computer Engineering (IJECE)***13**(2), 2177. (2023).
16. Jiang, C. et al. Xanthohumol inhibits TGF-β1-induced cardiac fibroblasts activation via mediating pten/akt/mtor signaling pathway. *Drug Des. Devel. Ther.***14**, 5431–5439. https://doi.org/10.2147/DDDT.S282206 (2020).
17. Azam, M. A. et al. A review on multimodal medical image fusion: Compendious analysis of medical modalities, multimodal databases, fusion techniques and quality metrics. *Comput. Biol. Med.***144**, 105253 (2022).
18. Liu, Q. et al. Weight status change during four years and left ventricular hypertrophy in Chinese children. *Front. Pead.* **12**, 1371286. https://doi.org/10.3389/fped.2024.1371286 (2024).
19. Yizheng Wang, Xin Zhang, Ying Ju, Qing Liu, Quan Zou, Yazhou Zhang, Yijie Ding, Ying Zhang. Identification of human microRNA-disease association via low-rank approximation-based link propagation and multiple kernel learning. *Front. of Comput. Sci.*. **18**(2), 182903 (2024).
20. Zhang, Z. et al. A case of pioneering subcutaneous implantable cardioverter defibrillator intervention in Timothy syndrome. *BMC Pediatr.***24**(1), 729. https://doi.org/10.1186/s12887-024-05216-w (2024).
21. Yu, H., Yang, L. T., Zhang, Q., Armstrong, D. & Deen, M. J. Convolutional neural networks for medical image analysis: State-of-the-art, comparisons, improvement and perspectives. *Neurocomputing***444**, 92–110 (2021).
22. Avendi, M. R., Kheradvar, A. & Jafarkhani, H. A combined deep-learning and deformable-model approach to fully automatic segmentation of the left ventricle in cardiac MRI. *Med. Image Anal.***30**, 108–119 (2016).
23. Bilal, H. et al. An intelligent approach for early and accurate predication of cardiac disease using hybrid artificial intelligence techniques. *Bioengineering***11**(12), 1290 (2024).
24. Manisha, M., Srivastava, S. & John, D. P. Heart disease predication using various machine learning algorithms. In *2024 International Conference on Healthcare Innovations, Software and Engineering Technologies (HISET)* 422–428 (IEEE., January.,2024)
25. Luan, S. et al. Deep learning for fast super-resolution ultrasound microvessel imaging. *Phys. Med. Biol.* **68** (24), 245023. https://doi.org/10.1088/1361-6560/ad0a5a (2023).
26. Ding, Z. et al. A supervised explainable machine learning model for perioperative neurocognitive disorder in Liver-Transplantation patients and external validation on the medical information Mart for intensive care IV database: retrospective study. *J. Med. Internet. Res.* **27** https://doi.org/10.2196/55046 (2025).
27. Qian, K. et al. Learning representations from heart sound: A comparative study on shallow anddeep models. *Cyborg Bionic Syst.* **5**, Article0075. https://doi.org/10.34133/cbsystems.0075 (2024).
28. Kothinti, R. R. Deep learning in healthcare: Transforming disease diagnosis, personalized treatment, and clinical decision-making through AI-driven innovations.. *World J. Adv. Res. Rev.*. **24**(2), 2841–2856 (2024).
29. Xia, L. X. et al. Exosomes derived from induced cardiopulmonary progenitor cells alleviate acute lung injury in mice. *Acta Pharmacol. Sin.***45**(8), 1644–1659. https://doi.org/10.1038/s41401-024-01253-4 (2024).
30. Singh, A., & Kumar, R. Heart disease prediction using machine learning algorithms. In *2020 international conference on electrical and electronics engineering (ICE3)*452-457 (IEEE,February,2020)
31. Lei, X. et al. Gli1 promotes epithelial-mesenchymal transition and metastasis of non-small cell lung carcinoma by regulating snail transcriptional activity and stability. *Acta Pharm. Sin. B***12**(10), 3877–3890. https://doi.org/10.1016/j.apsb.2022.05.024 (2022).
32. Babaei, H. et al. A machine learning model to estimate myocardial stiffness from EDPVR. *Sci. Rep.***12**(1), 5433 (2022).
33. Liao, Y., Tang, Z., Gao, K. & Trik, M. Optimization of resources in intelligent electronic health systems based on internet of things to predict heart diseases via artificial neural network. *Heliyon*https://doi.org/10.1016/j.heliyon.2024.e32090 (2024).
34. Mehdi, R. R. et al. Comparison of three machine learning methods to estimate myocardial stiffness. In Reduced order Models for the Biomechanics of Living Organs ;Academic.363–382. (2023).
35. Mehdi, R. R. et al. Non-Invasive diagnosis of chronic myocardial infarction via composite In-Silico-Human data learning. *Advanced Science*, e06933. (2025).
36. Wang, W. et al. Low-light image enhancement based on virtual exposure. *Sig. Process. Image Commun.* **118**, 117016. https://doi.org/10.1016/j.image.2023.117016 (2023).

37. Yin, L. et al. Convolution-Transformer for image feature extraction. *Comput. Model. Eng. Sci.* **141** (1), 87–106. https://doi.org/10.32604/cmes.2024.051083 (2024).
38. Rani, P. et al. An extensive review of machine learning and deep learning techniques on heart disease classification and prediction. *Arch. Comput. Methods Eng.* **31** (6), 3331–3349 (2024).
39. Yu, X. et al. Deep learning for fast denoising filtering in ultrasound localization microscopy. *Phys. Med. Biol.* **68** (20), 205002. https://doi.org/10.1088/1361-6560/acf98f (2023).
40. Abdar, M. et al. A new machine learning technique for an accurate diagnosis of coronary artery disease. *Comput. Methods Programs Biomed.***179**, 104992 (2019).
41. Yadav, S. S., Jadhav, S. M., Nagrale, S. & Patil, N. Application of machine learning for the detection of heart disease. In *2020 2nd international conference on innovative mechanisms for industry applications (ICIMIA)* 165–172. (IEEE., March ,2020)
42. Shorewala, V. Early detection of coronary heart disease using ensemble techniques. *Inf. Med. Unlocked*. **26**, 100655 (2021).
43. El-Ibrahimi, A. et al. A., Optimizing machine learning algorithms for heart disease classification and prediction. *International J. Online & Biomedical Engineering*, **19**(15). (2023).
44. Li, J. P. et al. Heart disease identification method using machine learning classification in e-healthcare. *IEEE Access***8**, 107562–107582 (2020).
45. Manimurugan, S., Almutairi, S., Aborokbah, M. M., Narmatha, C., Ganesan, S., Chilamkurti,N., … Almoamari, H. (2022). Two-stage classification model for the prediction of heart disease using IoMT and artificial intelligence. Sensors, 22(2), 476.
46. Ouyang, D. et al. Echonet-dynamic: a large new cardiac motion video data resource for medical machine learning. In *NeurIPS ML4H Workshop: Vancouver, BC, Canada* **5** (2019)
47. Nagavelli, U., Samanta, D. & Chakraborty, P. Machine learning technology-based heart disease detection models. *J. Healthc. Eng.* **2022** (1), 7351061 (2022).
48. Jindal, H., Agrawal, S., Khera, R., Jain, R. & Nagrath, P. Heart disease prediction using machine learning algorithms. In *IOP conference series: materials science and engineering.* **1022** (1) 012072 (IOP Publishing, 2021)
49. Chang, V., Bhavani, V. R., Xu, A. Q. & Hossain, M. A. An artificial intelligence model for heart disease detection using machine learning algorithms. *Healthcare Analytics***2**, 100016 (2022).

Author contributions
All authors conceived and designed the study. Tao Yu and KeYue Chen collected, simulated, and analyzed data. "KeYue Chen" wrote the first draft, and all authors reviewed it.

Funding
The authors did not receive any financial support for this study.

Declarations

Competing interests
The authors declare no competing interests.

Ethical approval
This study utilized the Cleveland Clinic Heart Patient Dataset sourced from the UCI Reference Website Dataset. This dataset is accessible to the public and can be utilized. https://archive.ics.uci.edu/ml/datasets/heart+Disease.

Consent to publish
No private dataset was used and therefore no consent to publish is required.

Additional information
Correspondence and requests for materials should be addressed to K.C.

Reprints and permissions information is available at www.nature.com/reprints.

Publisher's note Springer Nature remains neutral with regard to jurisdictional claims in published maps and institutional affiliations.